

UNCLASSIFIED

AD NUMBER

AD905676

LIMITATION CHANGES

TO:

Approved for public release; distribution is unlimited.

FROM:

Distribution authorized to U.S. Gov't. agencies only; Test and Evaluation; DEC 1972. Other requests shall be referred to Air Force Armament Lab., Eglin AFB, FL.

AUTHORITY

AFATL ltr 6 Feb 1979

THIS PAGE IS UNCLASSIFIED

AEDC-TR-72-182  
AFATL-TR-72-220

DEC 25 1972  
JAN 22 1973

cy.2



# SEPARATION TRAJECTORIES OF MODULAR WEAPON STORES WITH VARIOUS NOSE AND TAIL GEOMETRIES FROM THE F-4C AIRCRAFT

David W. Hill, Jr.

ARO, Inc.

December 1972

This document has been approved for public release  
its distribution is unlimited.

Distribution limited to U.S. Government agencies only;  
this report contains information on test and evaluation of  
military hardware; December 1972; other requests for this  
document must be referred to Air Force Armament  
Laboratory (DLJM), Eglin AFB, FL 32542

This document has been approved for public release

its distribution is unlimited. TAB 79.7 30 March 1979

**PROPULSION WIND TUNNEL FACILITY  
ARNOLD ENGINEERING DEVELOPMENT CENTER  
AIR FORCE SYSTEMS COMMAND  
ARNOLD AIR FORCE STATION, TENNESSEE**

# ***NOTICES***

When U. S. Government drawings specifications, or other data are used for any purpose other than a definitely related Government procurement operation, the Government thereby incurs no responsibility nor any obligation whatsoever, and the fact that the Government may have formulated, furnished, or in any way supplied the said drawings, specifications, or other data, is not to be regarded by implication or otherwise, or in any manner licensing the holder or any other person or corporation, or conveying any rights or permission to manufacture, use, or sell any patented invention that may in any way be related thereto.

Qualified users may obtain copies of this report from the Defense Documentation Center.

References to named commercial products in this report are not to be considered in any sense as an endorsement of the product by the United States Air Force or the Government.

**SEPARATION TRAJECTORIES OF MODULAR WEAPON  
STORES WITH VARIOUS NOSE AND TAIL  
GEOMETRIES FROM THE F-4C AIRCRAFT**

**David W. Hill, Jr.  
ARO, Inc.**

**Distribution limited to U.S. Government agencies only; this report contains information on test and evaluation of military hardware; December 1972; other requests for this document must be referred to Air Force Armament Laboratory (DLJM), Eglin AFB, FL 32542.**

## FOREWORD

The work reported herein was conducted by the Arnold Engineering Development Center (AEDC) under sponsorship of the Air Force Armament Laboratory (AFATL/DLG), Air Force Systems Command (AFSC), under Program Element 63601F, System 670D.

The test results presented were obtained by ARO, Inc. (a subsidiary of Sverdrup & Parcel and Associates, Inc.), contract operator of AEDC, AFSC, Arnold Air Force Station, Tennessee. The test was conducted from July 19 to August 2, 1972, under ARO Project No. PA021. The manuscript was submitted for publication on October 9, 1972.

This technical report has been reviewed and is approved.

L. R. KISSLING  
Lt Colonel, USAF  
Chief Air Force Test Director, PWT  
Directorate of Test

A. L. COAPMAN  
Colonel, USAF  
Director of Test

## ABSTRACT

Tests were conducted in the Aerodynamic Wind Tunnel (4T) using 0.05-scale models to investigate the separation characteristics of modular weapon configurations with different nose and tail geometries when released from various positions on the triple ejection rack at the wing inboard pylon location on the F-4C aircraft. Captive trajectory data were obtained for level flight at Mach numbers 0.6, 0.9, and 1.2 at a simulated altitude of 5000 ft. The parent aircraft angle of attack was varied from 0.1 to 2.4 deg, depending on Mach number. In general, for any nose and tail combination, the effect of increasing Mach number was to produce a more negative (nose down) initial pitch rate. For the configurations tested, and over the Mach number and trajectory intervals of this test, the modular weapon with a hemispherical nose and a conical boattail appeared to be the most suitable store for separation without store-to-parent contact.

Distribution limited to U.S. Government agencies only; this report contains information on test and evaluation of military hardware; December 1972; other requests for this document must be referred to Air Force Armament Laboratory (DLJM), Eglin AFB, FL 32542.

## CONTENTS

	<u>Page</u>
ABSTRACT . . . . .	iii
NOMENCLATURE . . . . .	vi
I. INTRODUCTION . . . . .	1
II. APPARATUS	
2.1 Test Facility . . . . .	1
2.2 Test Articles . . . . .	2
2.3 Instrumentation . . . . .	2
III: TEST DESCRIPTION	
3.1 Test Conditions . . . . .	3
3.2 Trajectory Data Acquisition . . . . .	3
3.3 Corrections . . . . .	4
3.4 Precision of Data . . . . .	4
IV. RESULTS AND DISCUSSION . . . . .	4

## APPENDIXES

### II. ILLUSTRATIONS

#### Figure

1. Isometric Drawing of a Typical Store Separation Installation and a Block Diagram of the Computer Control Loop . . . . .	9
2. Schematic of the Tunnel Test Section Showing Model Location . . . . .	10
3. Sketch of the F-4C Parent-Aircraft Model Showing Pylon Locations . . . . .	11
4. Details and Dimensions of the F-4C Inboard Pylon Model . . . . .	12
5. Details and Dimensions of the TER Model . . . . .	13
6. Details and Dimensions of Nose and Tail Combinations of Modular Weapons . . . . .	14
7. Photograph of Modular Weapons Models with Tail T4 and of the TER Model . . . . .	15
8. Details and Dimensions of the 370-gal Fuel Tank Model with Outboard Pylon . . . . .	16
9. Photograph Showing a Typical Model Installation for Store Separation Testing . . . . .	17
10. Ejector Force as a Function of Time for the TER and Pylon . . . . .	18
11. Schematic of the TER Store Stations and Orientations . . . . .	20
12. Effect of Nose Geometry Variation on the Separation Trajectories of the Modular Weapon Store with Tail T1, Configuration 1R . . . . .	21
13. Effect of Nose Geometry Variation on the Separation Trajectories of the Modular Weapon Store with Tail T2, Configuration 1R . . . . .	23
14. Effect of Nose Geometry Variation on the Separation Trajectories of the Modular Weapon Store with Tail T3, Configuration 1R . . . . .	25

<u>Figure</u>	<u>Page</u>
15. Effect of Nose Geometry Variation on the Separation Trajectories of the Modular Store with Tail T4, Configuration 1R . . . . .	27
16. Effect of Nose Geometry Variation on the Separation Trajectories of the Modular Weapon Stores with Tail T1, Configuration 1L . . . . .	29
17. Effect of Nose Geometry Variation on the Separation Trajectories of the Modular Weapon Stores with Tail T2, Configuration 1L . . . . .	31
18. Effect of Nose Geometry Variation on the Separation Trajectories of the Modular Weapon Stores with Tail T3, Configuration 1L . . . . .	33
19. Effect of Nose Geometry Variation on the Separation Trajectories of the Modular Weapon Stores with Tail T4, Configuration 1L . . . . .	35
20. Effect of Nose Geometry Variation on the Separation Trajectories of the Modular Weapon Stores with Tail T1, Configuration 2R . . . . .	37
21. Effect of Nose Geometry Variation on the Separation Trajectories of the Modular Weapon Stores with Tail T2, Configuration 2R . . . . .	39
22. Effect of Nose Geometry Variation on the Separation Trajectories of the Modular Weapon Stores with Tail T3, Configuration 2R . . . . .	41
23. Effect of Nose Geometry Variation on the Separation Trajectories of the Modular Weapon Stores with Tail T4, Configuration 2R . . . . .	43
24. Separation Trajectories of the Modular Weapon Store with Nose N1 and Tail T2 from the Inboard Pylon, Configuration 3R . . . . .	45

**II. TABLES**

I. Full-Scale Store Parameters Used in Trajectory Calculations . . . . .	47
II. Damping Coefficients Used in Trajectory Calculations . . . . .	48
III. Axial-Force Coefficients, $C_A$ , Used in Full-Scale Trajectory Calculations . . . . .	48
IV. F-4C Load Configurations . . . . .	49

**NOMENCLATURE**

<b>BL</b>	Aircraft buttock line from plane of symmetry, in., model scale
<b>b</b>	Store reference dimension, ft full scale
<b><math>C_A</math></b>	Store axial-force coefficient, axial force/ $q_\infty S$
<b><math>C_l</math></b>	Store rolling-moment coefficient, rolling moment/ $q_\infty S b$
<b><math>C_{l_p}</math></b>	Store roll-damping derivative, $dC_l/d(pb/2V_\infty)$
<b><math>C_m</math></b>	Store pitching-moment coefficient, referenced to the store cg, pitching moment/ $q_\infty S b$

$C_{m_q}$	Store pitch-damping derivative, $dC_m/d(qb/2V_\infty)$
$C_n$	Store yawing-moment coefficient, referenced to the store cg, yawing moment/ $q_\infty S b$
$C_{n_r}$	Store yaw-damping derivative, $dC_n/d(rb/2V_\infty)$
FS	Aircraft fuselage station, in., model scale
$F_Z$	MER/TER ejector force, lb
$F_{Z_1}$	Pylon forward ejector force, lb
$F_{Z_2}$	Pylon aft ejector force, lb
H	Pressure altitude, ft
$I_{yy}$	Full-scale moment of inertia about the store $Y_B$ axis, slug-ft <sup>2</sup>
$I_{zz}$	Full-scale moment of inertia about the store $Z_B$ axis, slug-ft <sup>2</sup>
$M_\infty$	Free-stream Mach number
$\bar{m}$	Full-scale store mass, slugs
$p$	Store angular velocity about the $X_B$ axis, radians/sec
$q$	Store angular velocity about the $Y_B$ axis, radians/sec
$q_\infty$	Free-stream dynamic pressure, psf
$r$	Store angular velocity about the $Z_B$ axis, radians/sec
S	Store reference area, ft <sup>2</sup> , full scale
t	Real trajectory time from initiation of trajectory, sec
$V_\infty$	Free-stream velocity, ft/sec
WL	Aircraft waterline from reference horizontal plane, in., model scale
X	Separation distance of the store cg parallel to the flight axis system $X_F$ direction, ft, full scale measured from the prelaunch position
$X_{cg}$	Full-scale cg location, ft from nose of store

- $X_L$  Ejector piston location relative to the store cg, positive forward of store cg, ft, full scale
- $X_{L_1}$  Forward ejector piston location relative to the store cg, positive forward of store cg, ft, full scale
- $X_{L_2}$  Aft ejector piston location relative to the store cg, positive forward of store cg, ft, full scale
- $Y$  Separation distance of the store cg parallel to the flight axis system  $Y_F$  direction, ft, full scale measured from the prelaunch position
- $Z$  Separation distance of the store cg parallel to the flight-axis system  $Z_F$  direction, ft, full scale measured from the prelaunch position
- $ZE$  Ejector stroke length, ft, full scale
- $\alpha$  Parent-aircraft model angle of attack relative to the free-stream velocity vector, deg
- $\theta$  Angle between the store longitudinal axis and its projection in the  $X_F - Y_F$  plane, positive when store nose is raised as seen by pilot, deg
- $\psi$  Angle between the projection of the store longitudinal axis in the  $X_F - Y_F$  plane and the  $X_F$  axis, positive when the store nose is to the right as seen by the pilot, deg

**FLIGHT-AXIS SYSTEM COORDINATES**

**Directions**

- $X_F$  Parallel to the free-stream wind vector, positive direction is forward as seen by the pilot
- $Y_F$  Perpendicular to the  $X_F$  and  $Z_F$  directions, positive direction is to the right as seen by the pilot
- $Z_F$  In the aircraft plane of symmetry, perpendicular to the free-stream wind vector, positive direction is downward

The flight-axis system origin is coincident with the aircraft cg and remains fixed with respect to the parent aircraft during store separation. The  $X_F$ ,  $Y_F$ , and  $Z_F$  coordinate axes do not rotate with respect to the initial flight direction and attitude.

## STORE BODY-AXIS COORDINATES

### Directions

- $X_B$  Parallel to the store longitudinal axis, positive direction is upstream in the prelaunch position
- $Y_B$  Perpendicular to the store longitudinal axis, and parallel to the flight-axis system  $X_F - Y_F$  plane when the store is at zero roll angle, positive direction is to the right looking upstream when the store is at zero yaw and roll angles
- $Z_B$  Perpendicular to both the  $X_B$  and  $Y_B$  axes, positive direction is downward as seen by the pilot when the store is at zero pitch and roll angles.

The store body-axis system origin is coincident with the store cg and moves with the store during separation from the parent airplane. The  $X_B$ ,  $Y_B$ , and  $Z_B$  coordinate axes rotate with the store in pitch, yaw, and roll so that mass moments of inertia about the three axes are not time-varying quantities.

## SECTION I INTRODUCTION

The work reported herein pertains to the modular weapon program being sponsored by the Air Force Armament Laboratory (AFATL). The objective of this phase of the program is to aerodynamically design an 800-lb bomb using modular components such that, over a range of test conditions, it would release safely from the aircraft and would follow trajectories for high targeting accuracy. After the design is verified by wind tunnel tests, the internal package of the bomb would be designed.

To determine the separation characteristics of some proposed modular weapon shapes, 0.05-scale models of the F-4C aircraft and the various store shapes were employed in a captive trajectory test conducted in the Aerodynamic Wind Tunnel (4T). Data were obtained for releases from the inboard pylon and from the triple ejection rack on the inboard pylon. The flight conditions simulated were level flight at Mach numbers of 0.6, 0.9, and 1.2 and at a pressure altitude of 5000 ft. The ejector forces used were time-variant functions provided by the Air Force Armament Laboratory.

## SECTION II APPARATUS

### 2.1 TEST FACILITY

The Aerodynamic Wind Tunnel (4T) is a closed-loop, continuous flow, variable-density tunnel in which the Mach number can be varied from 0.1 to 1.3. At all Mach numbers, the stagnation pressure can be varied from 300 to 3700 psfa. The test section is 4 ft square and 12.5 ft long with perforated, variable porosity (0.5- to 10-percent open) walls. It is completely enclosed in a plenum chamber from which the air can be evacuated, allowing part of the tunnel airflow to be removed through the perforated walls of the test section.

For store separation testing, two separate and independent support systems are used to support the models. The parent aircraft model is inverted in the test section and supported by an offset sting attached to the main pitch sector. The store model is supported by the captive trajectory support (CTS) which extends down from the tunnel top wall and provides store movement (six degrees of freedom) independent of the parent-aircraft model. An isometric drawing of a typical store separation installation is shown in Fig. 1, Appendix I.

Also shown in Fig. 1 is a block diagram of the computer control loop used during captive trajectory testing. The analog system and the digital computer work as an integrated unit and, utilizing required input information, control the store movement during a trajectory. Store positioning is accomplished by use of six individual d-c electric motors. Maximum translational travel of the CTS is  $\pm 15$  in. from the tunnel centerline in the lateral and vertical directions and 36 in. in the axial direction. Maximum angular

displacements are  $\pm 45$  deg in pitch and yaw and  $\pm 360$  deg in roll. A more complete description of the test facility can be found in the Test Facilities Handbook.<sup>1</sup> A schematic showing the test section details and the location of the models in the tunnel is shown in Fig. 2.

## 2.2 TEST ARTICLES

The test articles were 0.05-scale models of the F-4C parent aircraft and the various store shapes. A sketch showing the basic dimensions of the F-4C parent model is shown in Fig. 3. Details and dimensions of the inboard pylon and the triple ejection rack (TER) are shown in Figs. 4 and 5, respectively, and the store models are shown in Figs. 6, 7, and 8. There were three nose sections, one center section, and four tail sections, interchangeable for a total of 12 modular weapon configurations.

The F-4C parent model was geometrically similar to the full-scale airplane except for some modifications incident to the wind tunnel installation and CTS operation. Horizontal and vertical tail surfaces were removed because of interference with the CTS support. The parent model was inverted in the tunnel and attached by a 19-deg offset sting to the main sting support system (Fig. 2). Figure 9 shows a typical tunnel installation photograph of the parent aircraft and a store model.

The F-4C aircraft has two pylon stations on each wing. The mounting surface on the inboard pylon is 1 deg nose down with respect to the aircraft waterline. The fuel tank is mounted on the outboard pylon with a 1.5-deg nose down attitude.

The store models were mounted on an internal balance with an integral sting. The sting was in turn connected to the CTS support by means of a 3.-in. offset adapter.

## 2.3 INSTRUMENTATION

A five-component internal strain-gage balance was used to obtain the force and moment data on the store models. Translational and angular positions of the store models were obtained from the CTS analog outputs. The parent aircraft angle of attack was set using the main sting support and readout system. The CTS was electrically connected to automatically stop and give a visual indication if the store model or sting contacted the parent-aircraft surface. Spring-loaded plungers were located in the pylons and TER in order to provide a position indication when the store model was in the carriage position. The plunger circuit was independent of the parent-aircraft grounding circuit.

---

<sup>1</sup>Test Facilities Handbook (Ninth Edition). "Propulsion Wind Tunnel Facility, Vol. 4." Arnold Engineering Development Center, July 1971.

## SECTION III TEST DESCRIPTION

### 3.1 TEST CONDITIONS

Separation trajectory data were obtained at Mach numbers from 0.6 to 1.2. Tunnel dynamic pressure was 500 psf, and tunnel stagnation temperature was maintained near 100°F.

Tunnel conditions were held constant at the desired Mach number and stagnation pressure while data for each trajectory were obtained. The trajectories were terminated when the store or sting contacted the parent-aircraft model or when a CTS limit was reached.

### 3.2 TRAJECTORY DATA ACQUISITION

To obtain a trajectory, test conditions were established in the tunnel and the parent model was positioned at the desired angle of attack. The store model was then oriented to a position corresponding to the store carriage location. After the store was set at the desired initial position, operational control of the CTS was switched to the digital computer which controlled the store movement during the trajectory through commands to the CTS analog system (see block diagram, Fig. 1). Data from the wind tunnel, consisting of measured model forces and moments, wind tunnel operating conditions, and CTS rig positions, were input to the digital computer for use in the full-scale trajectory calculations.

The digital computer was programmed to solve the six-degree-of-freedom equations to calculate the angular and linear displacements of the store relative to the parent aircraft pylon. In general, the program involves using the last two successively measured values of each static aerodynamic coefficient to predict the magnitude of the coefficients over the next time interval of the trajectory. These predicted values are used to calculate the new position and attitude of the store at the end of the time interval. The CTS is then commanded to move the store model to this new position and the aerodynamic loads are measured. If these new measurements agree with the predicted values, the process is continued over another time interval of the same magnitude. If the measured and predicted values do not agree within the desired precision, the calculation is repeated over a time interval one-half the previous value. This process is repeated until a complete trajectory has been obtained.

In applying the wind tunnel data to the calculations of the full-scale store trajectories, the measured forces and moments are reduced to coefficient form and then applied with proper full-scale store dimensions and flight dynamic pressure. Dynamic pressure was calculated using a flight velocity equal to the free-stream velocity component plus the components of store velocity relative to the aircraft, and a density corresponding to the simulated altitude.

The initial portion of each launch trajectory incorporated simulated ejector forces in addition to the measured aerodynamic forces acting on the store. The ejector force functions for the stores are presented in Fig. 10. The ejector force was considered to act perpendicular to the rack or pylon mounting surface. The locations of the applied ejector forces and other full-scale store parameters used in the trajectory calculations are listed in Table I, Appendix II.

### 3.3 CORRECTIONS

Balance, sting, and support deflections caused by the aerodynamic loads on the store models were accounted for in the data reduction program to calculate the true store-model angles. Corrections were also made for model weight tares to calculate the net aerodynamic forces on the store model.

### 3.4 PRECISION OF DATA

The trajectory data are subject to error resulting from uncertainties in tunnel conditions, balance measurements, extrapolation tolerances, and CTS positioning control. Maximum error in the CTS position control was  $\pm 0.05$  in. for translational settings and  $\pm 0.15$  deg for angular displacements in pitch and yaw. Extrapolation tolerances were  $\pm 0.1$  for all aerodynamic coefficients. Based on a 95-percent confidence level, and ignoring bias errors, the uncertainties in the full-scale trajectory data resulting from balance inaccuracies are:

<u>M<sub>∞</sub></u>	<u>Time</u>	<u>ΔY</u>	<u>ΔZ</u>	<u>Δθ</u>	<u>Δψ</u>
0.6	0.2	±0.007	±0.007	±0.11	±0.11
	0.4	±0.03	±0.03	±0.46	±0.46
1.2	0.2	±0.03	±0.03	±0.46	±0.46

Estimated uncertainty in setting Mach number was  $\pm 0.003$ , and the uncertainty in aircraft model angle of attack was estimated to be  $\pm 0.1$  deg.

## SECTION IV RESULTS AND DISCUSSION

Data taken during the test consisted of ejector-separated trajectories of various store configurations from the inboard pylon and the TER on the wing of the F-4C aircraft. Data showing the linear displacements of the store relative to the carriage position and angular displacements relative to the flight-axis coordinate system are presented as functions of full-scale trajectory time in Figs. 12 through 24. Although rolling moments were measured on the stores for each trajectory, roll position data are not presented because the angle changes were small. Tables I through III list some of the parameters used in the trajectory calculations, and Table IV illustrates the F-4C load configurations.

Separation trajectory data of the modular weapon stores are presented in the following order: Figures 12 through 15 present separation trajectory data from TER station 2 on the right wing (configuration 1R) with a dummy store on TER station 3; Figures 16 through 19 present separation trajectory data from TER station 2 on the left wing (configuration 1L) with no dummy stores on the TER; Figures 20 through 23 present separation trajectory data from TER station 1 from the right wing (configuration 2R) with two dummy stores on the TER; and Figure 24 presents separation trajectory data from the right-wing inboard pylon (configuration 3R).

In general, increasing the Mach number increased the nose down pitch rate for all the stores. Data are presented in Figs. 12 through 24 only for the minimum and maximum Mach numbers for each configuration.

For the configurations tested, and over the Mach number and trajectory intervals of this test, the modular weapon configuration with nose and tail combination T2N1 appeared to be most suitable store for separation without store-to-parent contact.

In general, there was little effect on the translational motion of the stores from varying the nose shape for a given tail shape, and the trend of the angular motion was the same in each case.

The separation trajectories of configuration T2N1 from the inboard pylon showed an increase both in nose down pitch rate and nose inboard yaw rate with an increase in Mach number. The vertical separation rate was increased only slightly.

**APPENDIXES**  
**I. ILLUSTRATIONS**  
**II. TABLES**

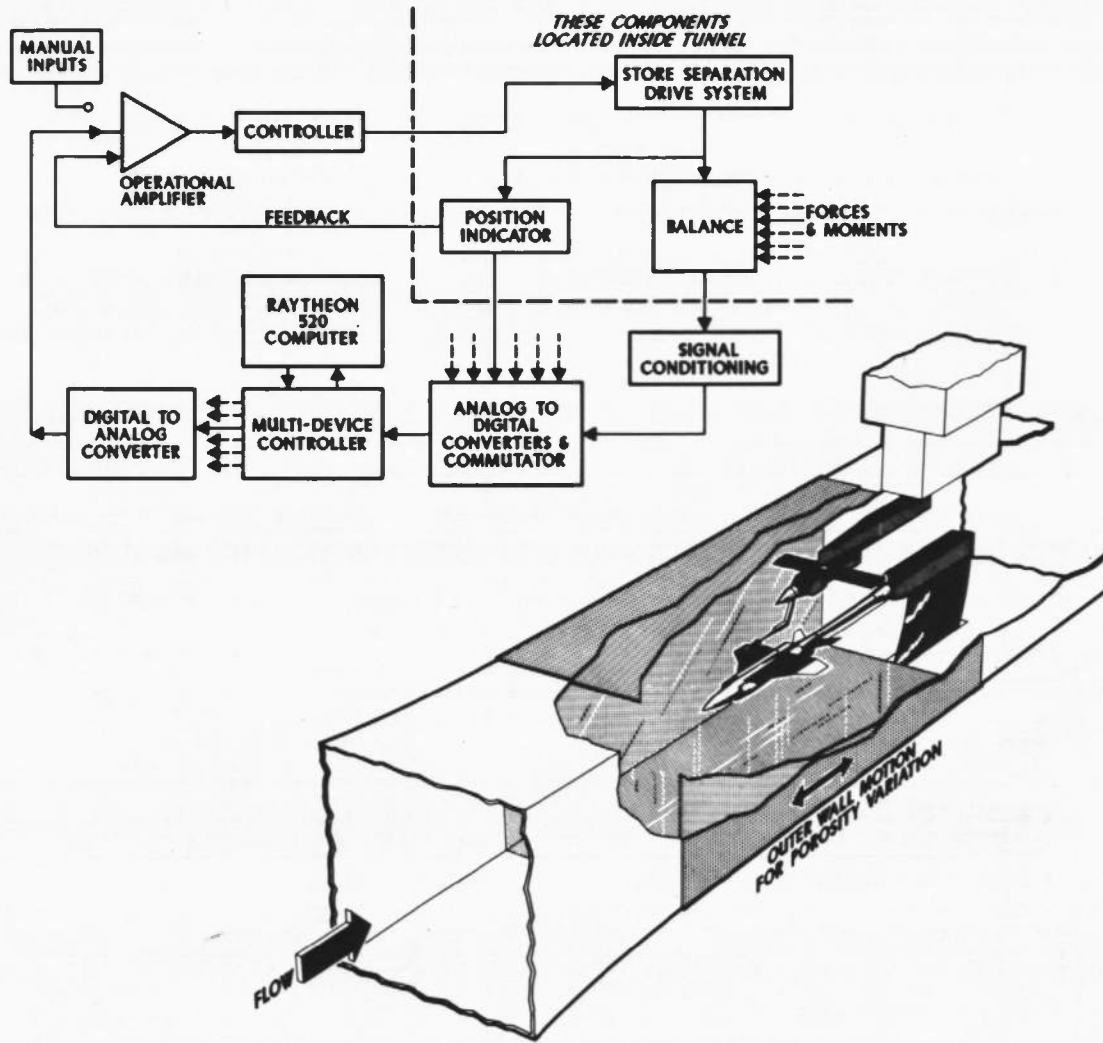
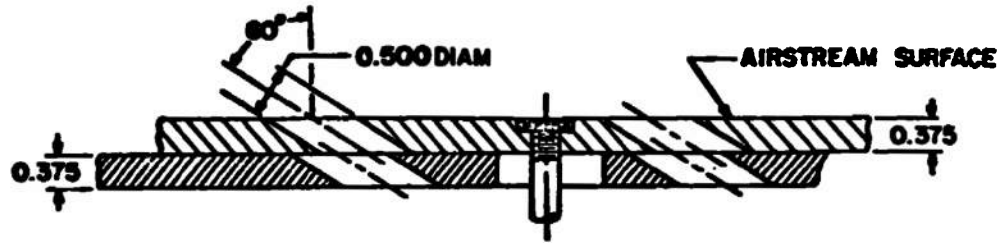


Fig. 1 Isometric Drawing of a Typical Store Separation Installation and a Block Diagram of the Computer Control Loop



TYPICAL PERFORATED WALL CROSS SECTION

TUNNEL STATIONS AND DIMENSIONS ARE IN INCHES

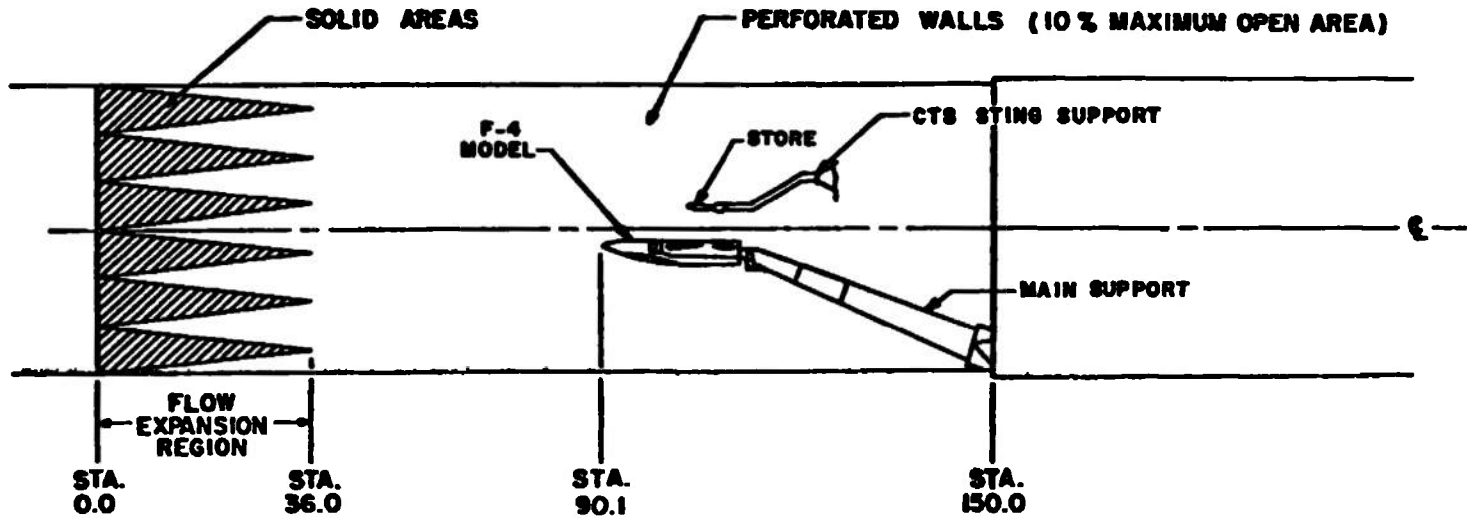
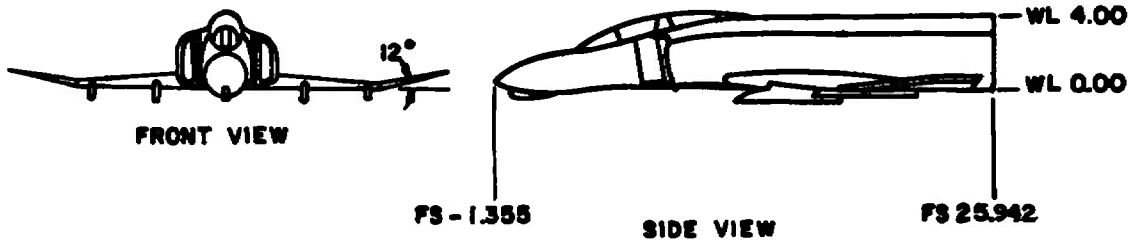


Fig. 2 Schematic of the Tunnel Test Section Showing Model Location



ALL DIMENSIONS IN INCHES

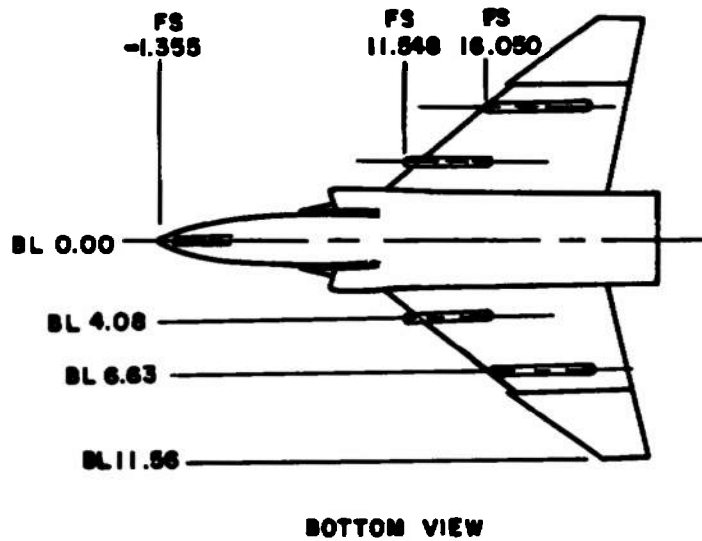
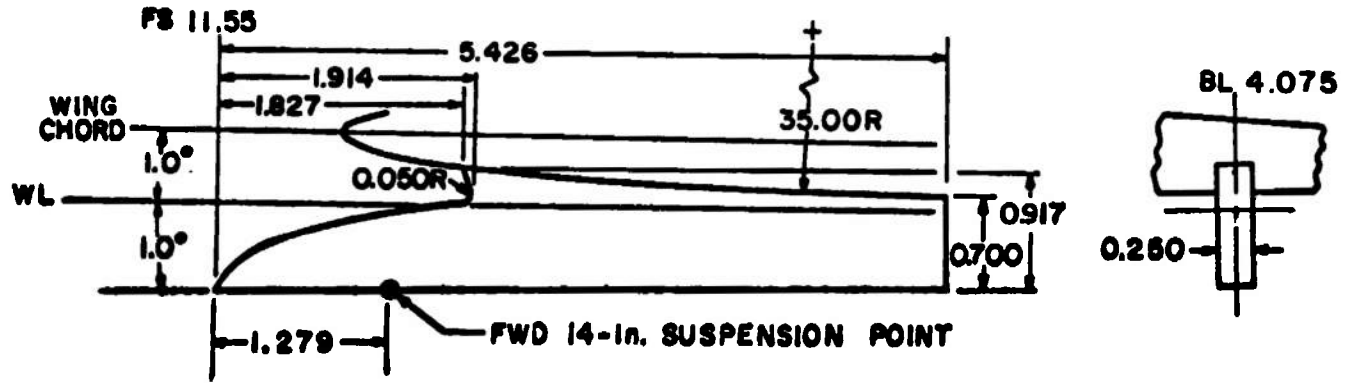


Fig. 3 Sketch of the F-4C Parent-Aircraft Model Showing Pylon Locations



ALL DIMENSIONS IN INCHES

Fig. 4 Details and Dimensions of the F-4C Inboard Pylon Model

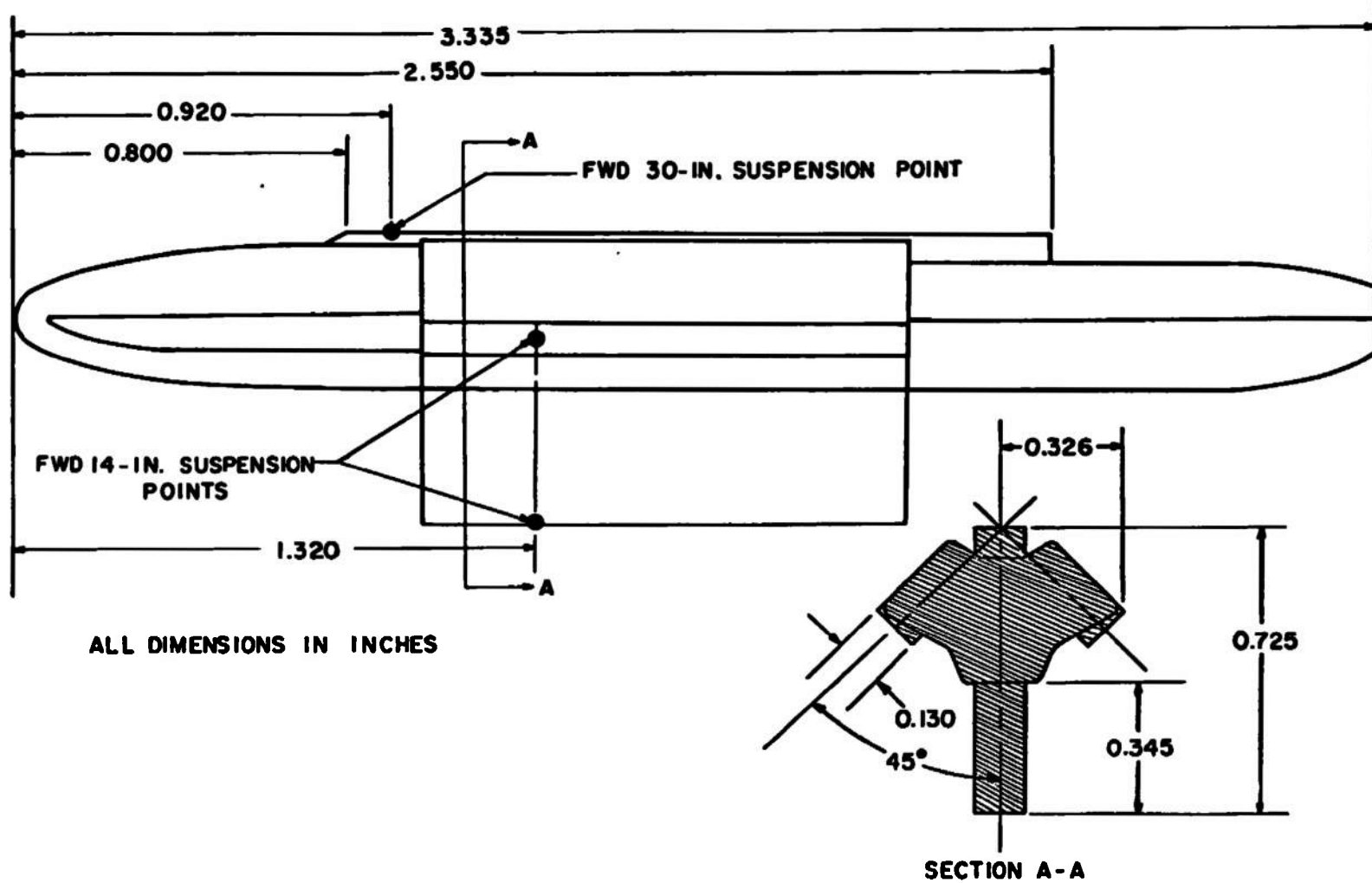


Fig. 5 Details and Dimensions of the TER Model

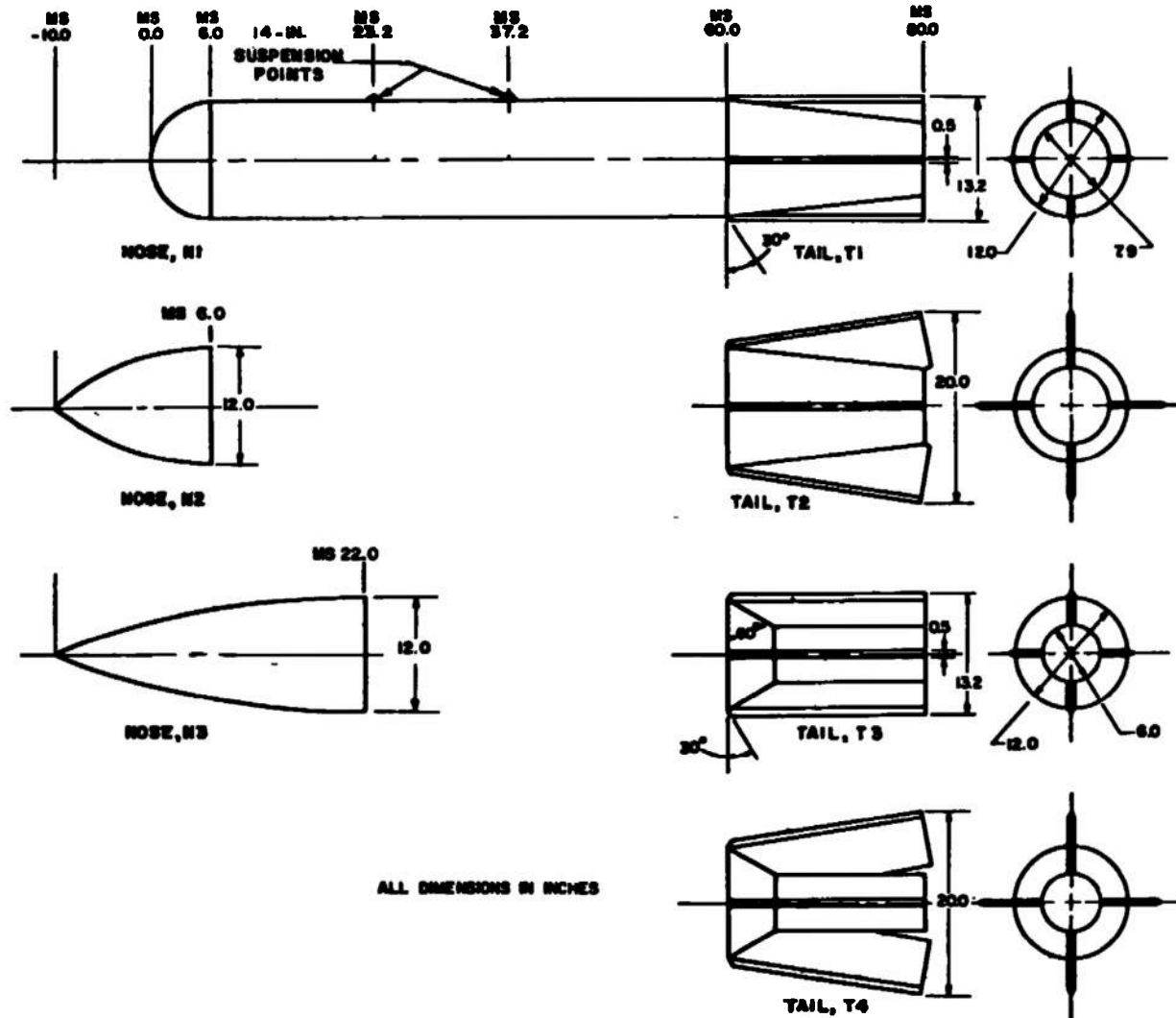
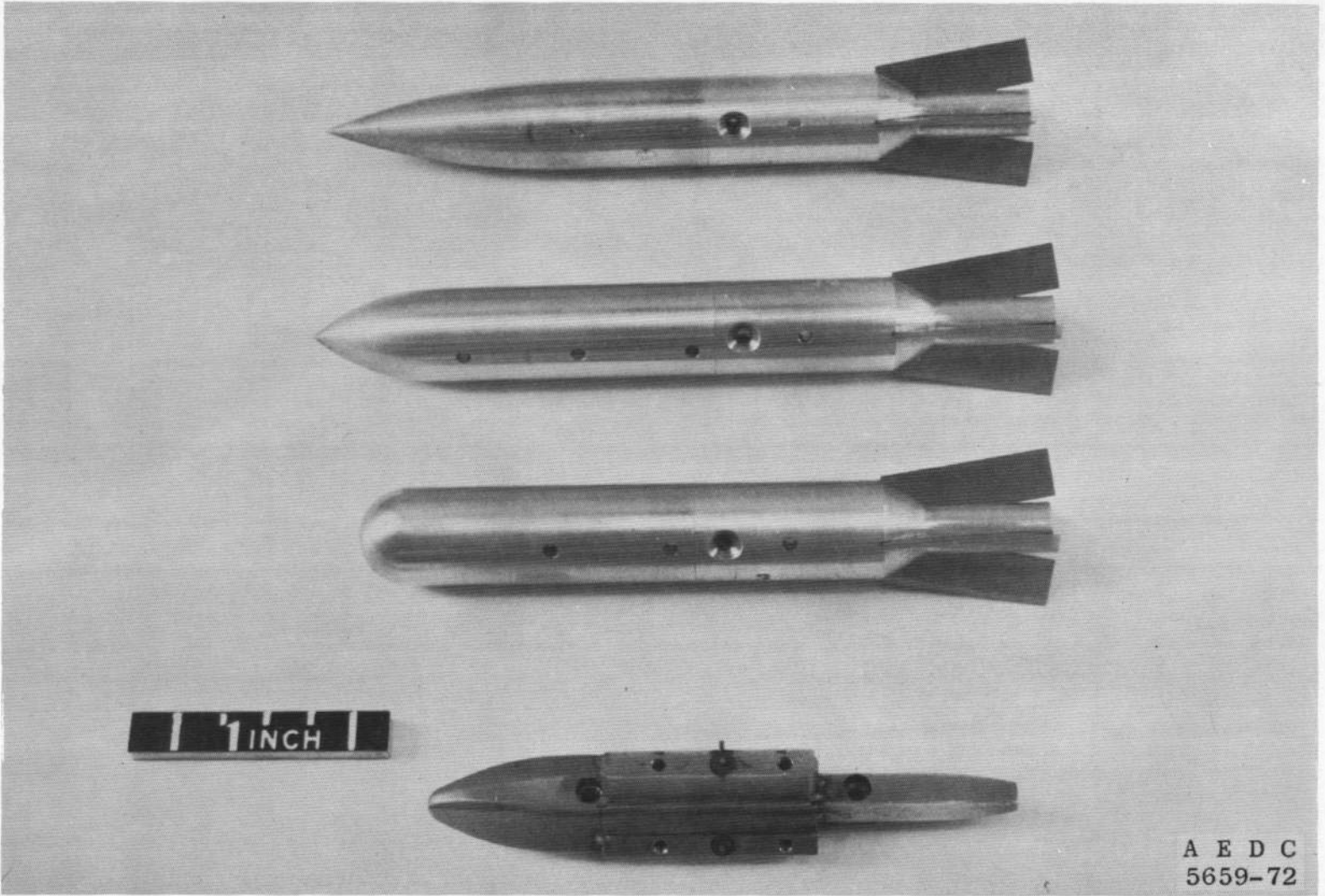
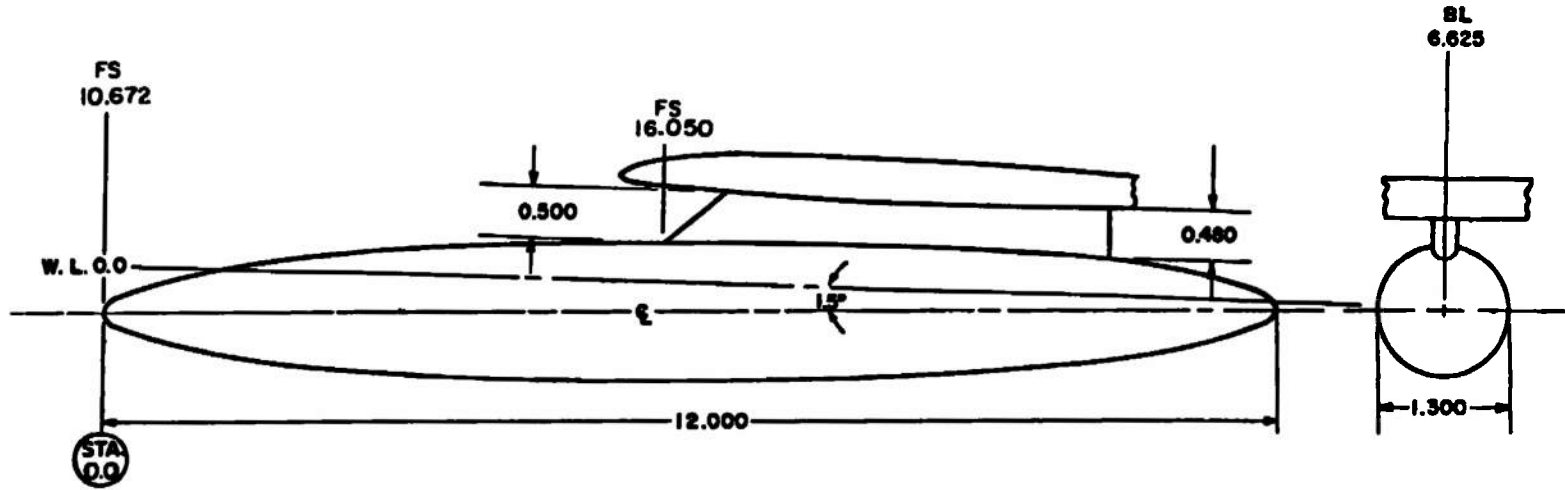


Fig. 6 Details and Dimensions of Nose and Tail Combinations of Modular Weapons



A E D C  
5659-72

Fig. 7 Photograph of Modular Weapons Models with Tail T4 and of the TER Model



NOTE: MODEL STATIONS AND DIMENSIONS IN INCHES

BODY CONTOUR, TYPICAL BOTH ENDS

STATION	BODY DIAM	STATION	BODY DIAM
0.000	0.000	2.500	1.116
0.025	0.100	2.750	1.156
0.050	0.144	3.000	1.190
0.150	0.258	3.250	1.218
0.250	0.340	3.500	1.242
0.500	0.498	3.750	1.260
0.750	0.622	4.000	1.274
1.000	0.724	4.250	1.286
1.250	0.812	4.500	1.294
1.500	0.890	4.750	1.298
1.750	0.958	5.000	1.300
2.000	1.016	6.000	1.300
2.250	1.070		

Fig. 8 Details and Dimensions of the 370-gal Fuel Tank Model with Outboard Pylon

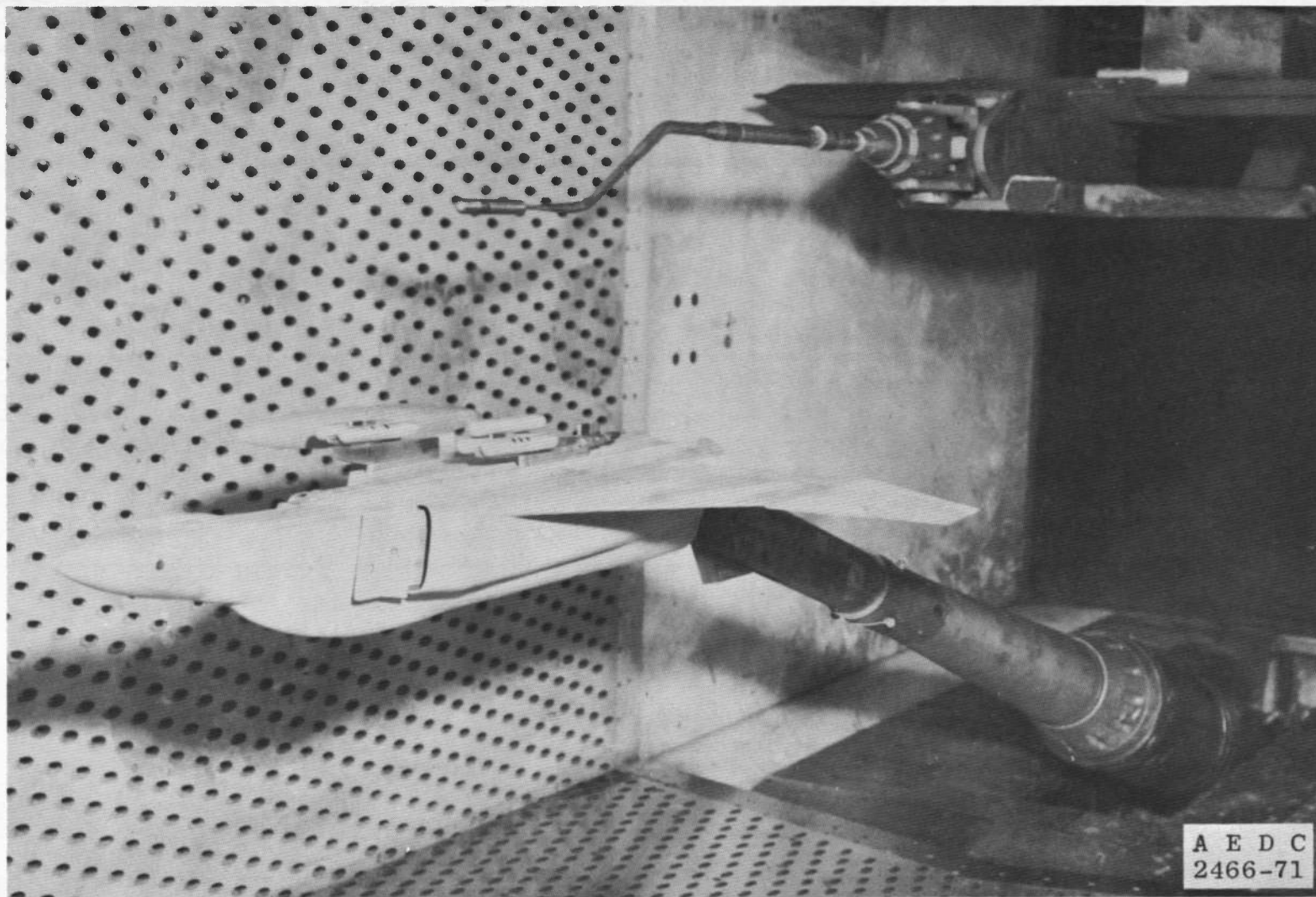


Fig. 9 Photograph Showing a Typical Model Installation for Store Separation Testing

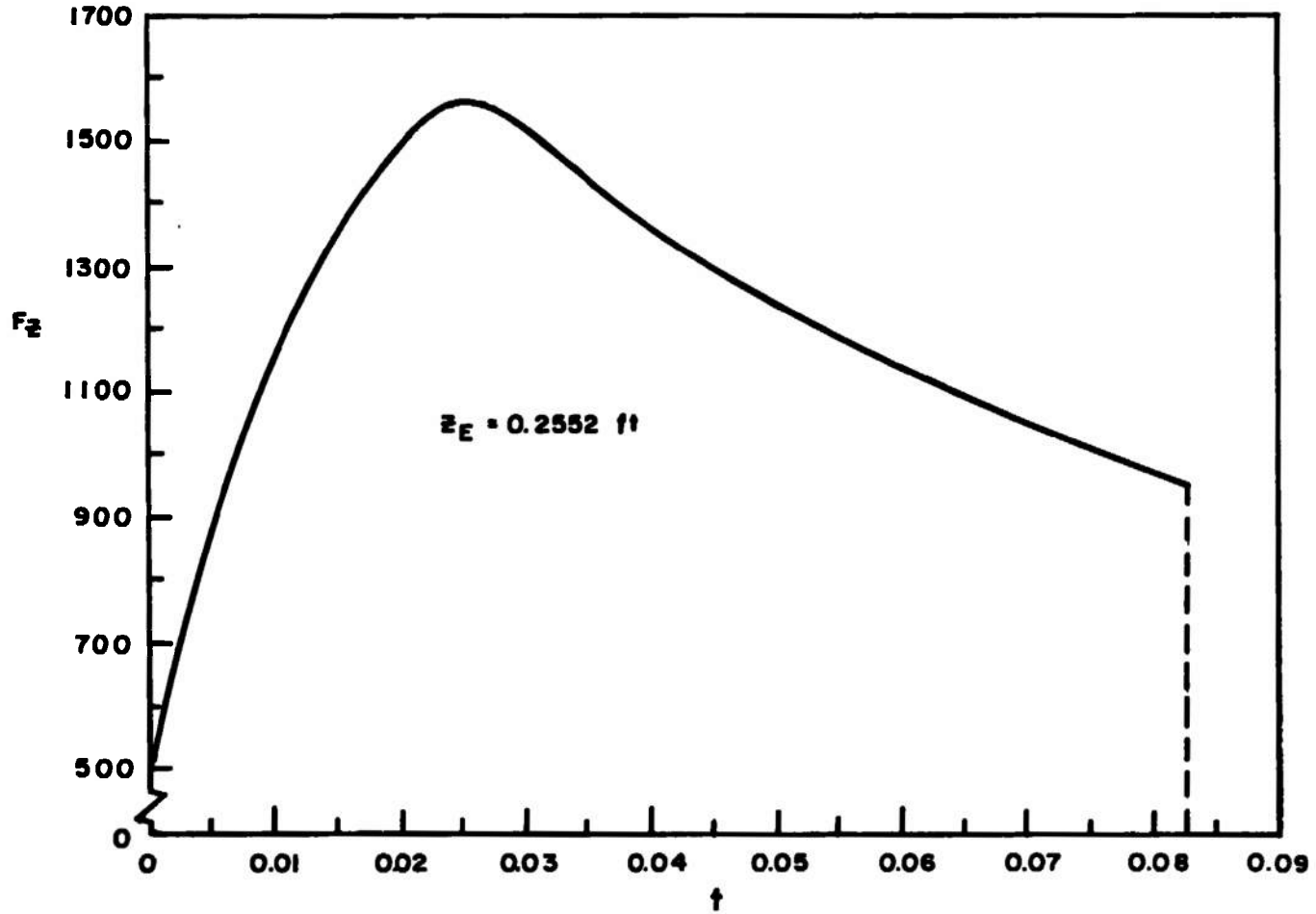


Fig. 10 Ejector Force as a Function of Time for the TER and Pylon

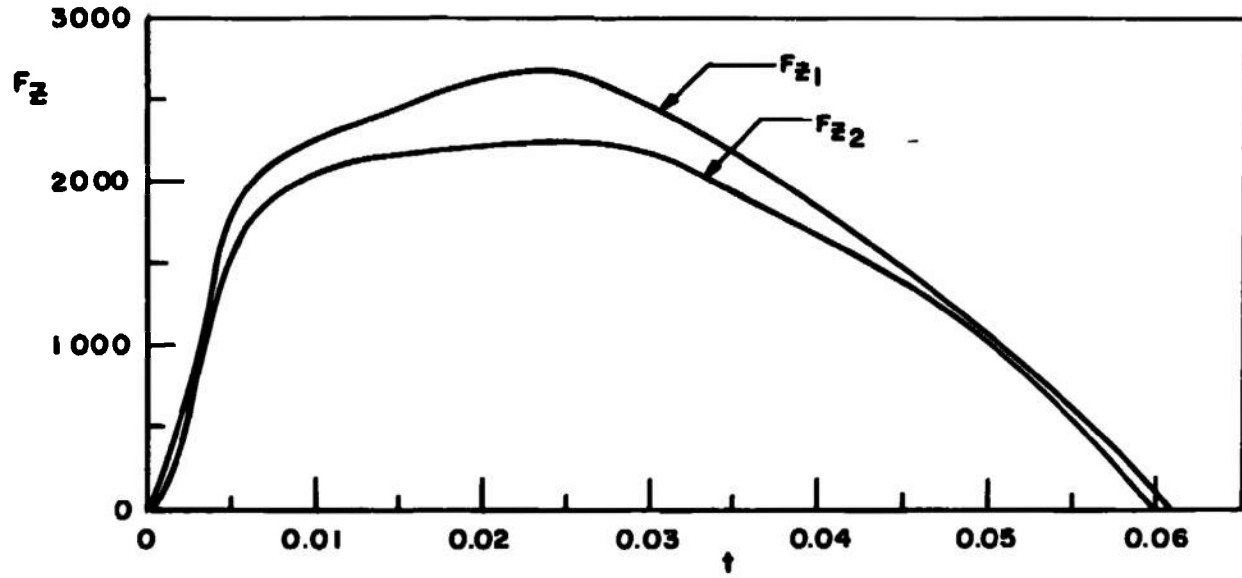
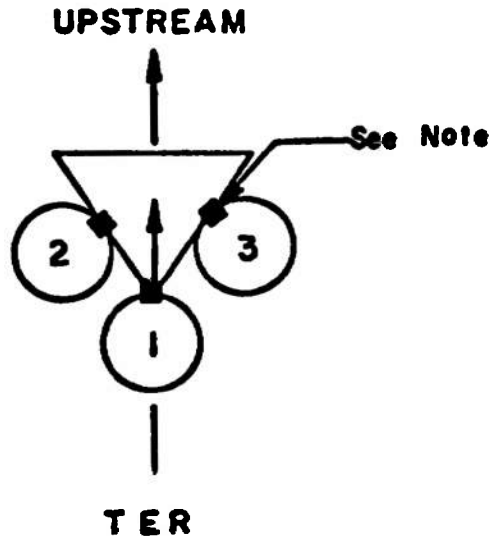


Fig. 10 Concluded

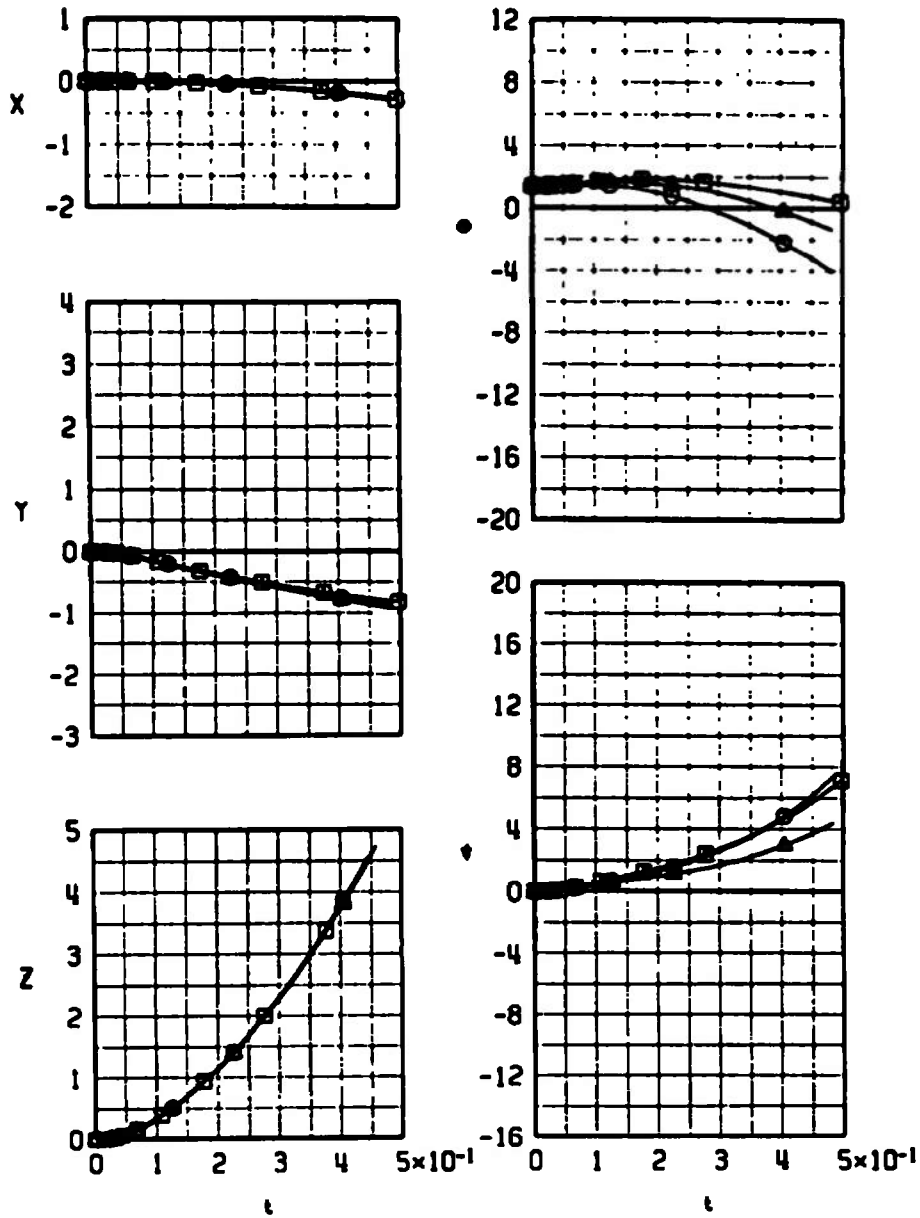


**NOTE:** The square indicates the orientation of the suspension lugs.

STATION	ROLL ORIENTATION,deg
1	0
2	45
3	-45

**Fig. 11 Schematic of the TER Store Stations and Orientations**

SYMBOL	$M_\infty$	$\alpha$	MODEL
□	0.60	2.4	T1-N1
○	0.60	2.4	T1-N2
△	0.60	2.4	T1-N3

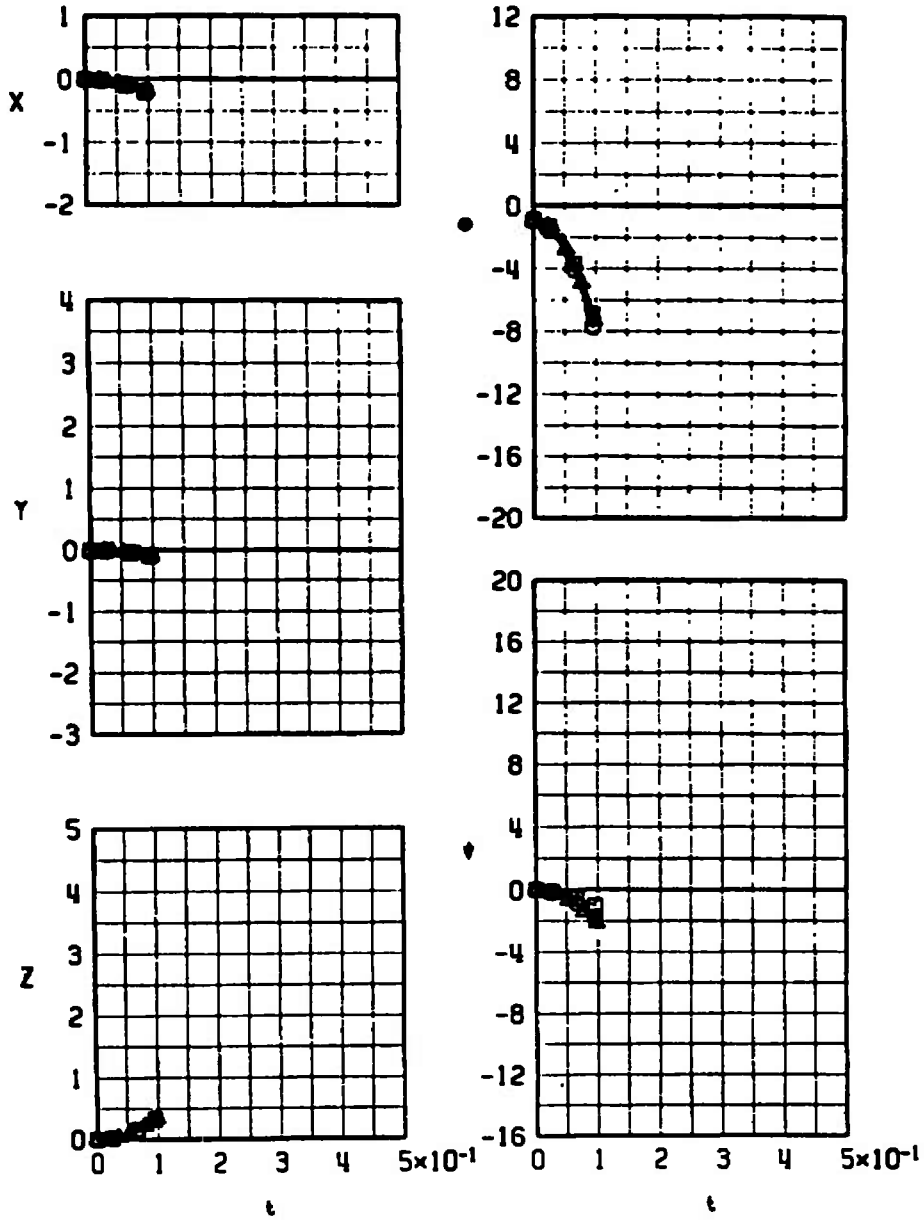


a.  $M_\infty = 0.60$

Fig. 12 Effect of Nose Geometry Variation on the Separation Trajectories of the Modular Weapon Store with Tail T1, Configuration 1R

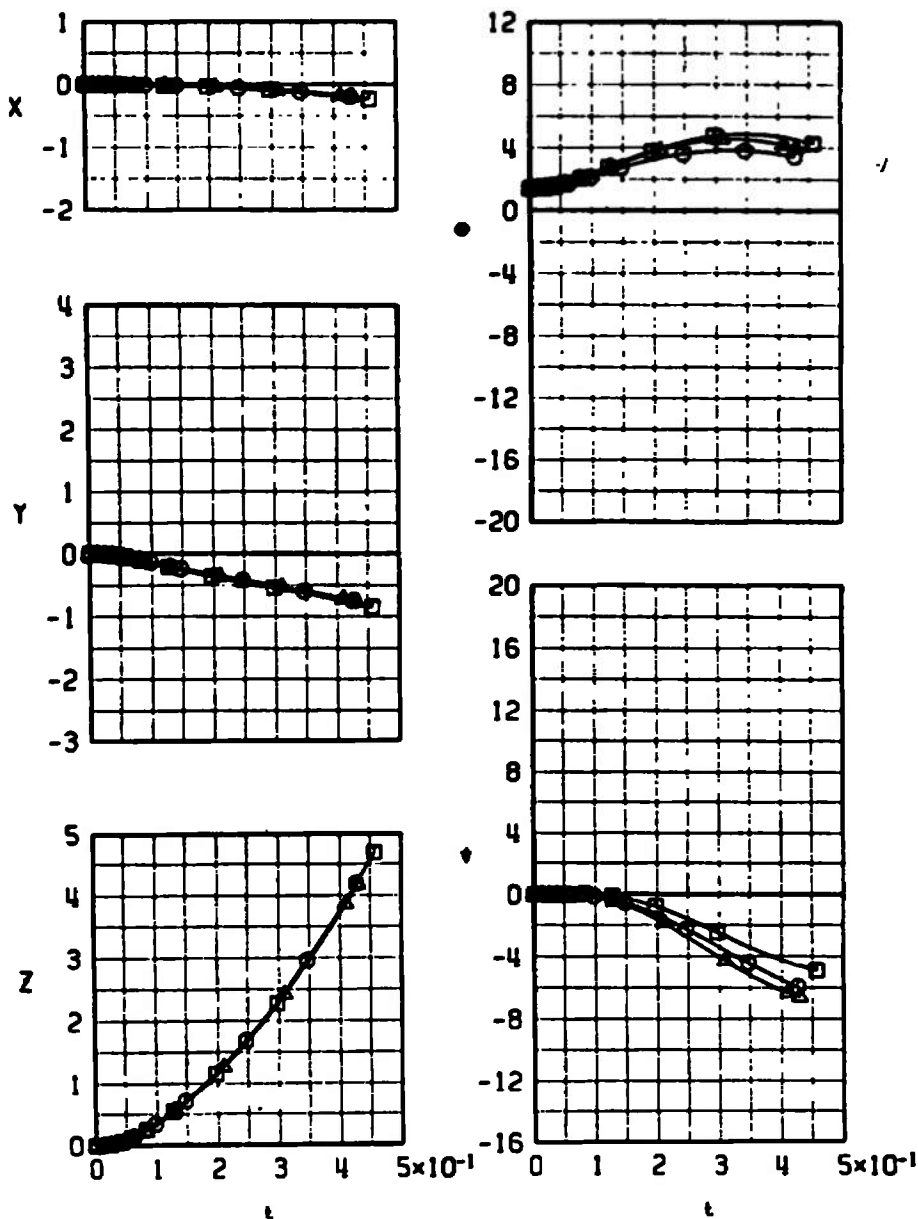
SYMBOL	$M_\infty$	$\alpha$	MODEL
□*	1.20	0.1	T1-N1
○*	1.20	0.1	T1-N2
△*	1.20	0.1	T1-N3

\* STORE-TO-PARENT CONTACT



b.  $M_\infty = 1.20$   
 Fig. 12 Concluded

SYMBOL	$M_\infty$	$\alpha$	MODEL
□	0.60	2.4	T2-N1
○	0.60	2.4	T2-N2
△	0.60	2.4	T2-N3

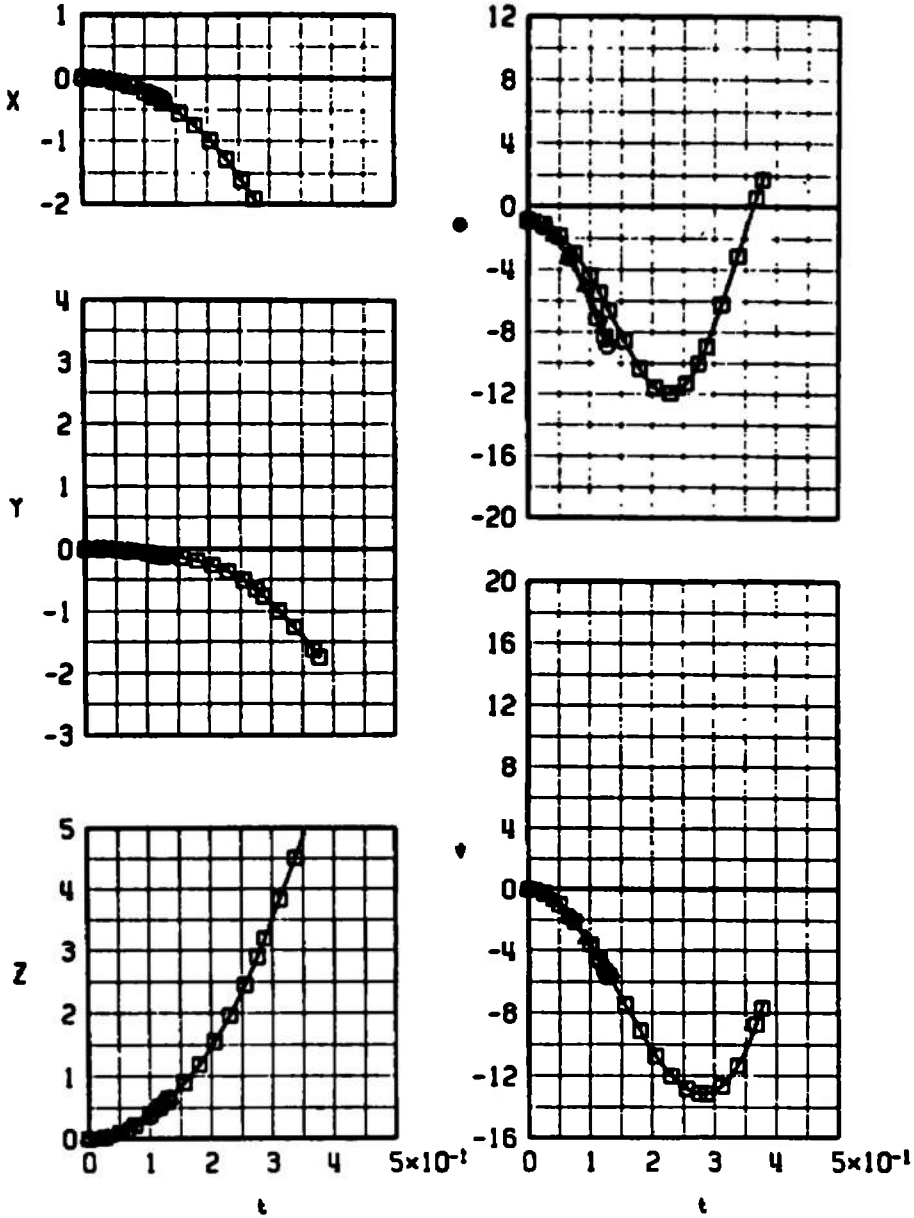


a.  $M_\infty = 0.60$

Fig. 13 Effect of Nose Geometry Variation on the Separation Trajectories of the Modular Weapon Store with Tail T2, Configuration 1R

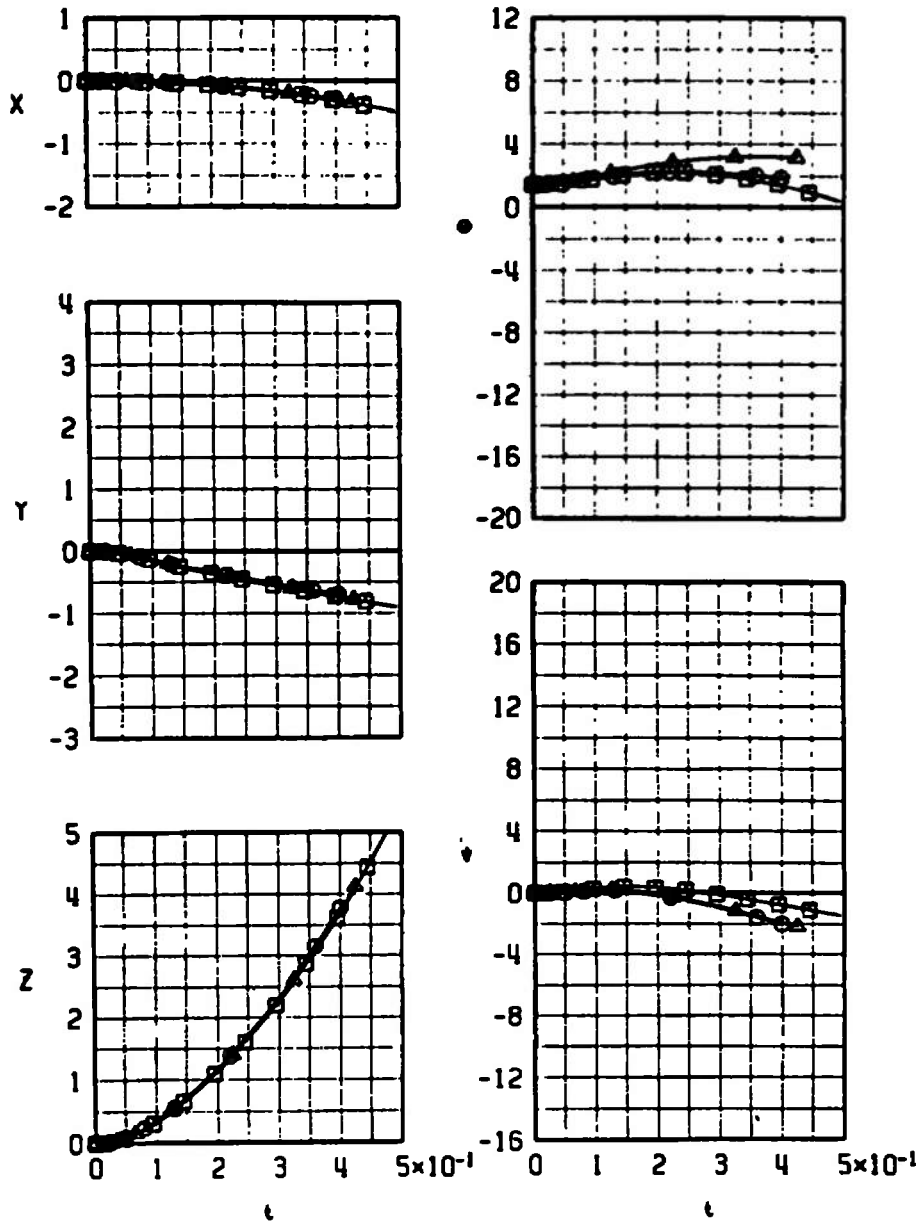
SYMBOL	$M_\infty$	$\alpha$	MODEL
□	1.20	0.1	T2-N1
○*	1.20	0.1	T2-N2
△*	1.20	0.1	T2-N3

\* STORE-TO-PARENT CONTACT



b.  $M_\infty = 1.20$   
 Fig. 13 Concluded

SYMBOL	$M_\infty$	$\alpha$	MODEL
□	0.60	2.4	T3-N1
○	0.60	2.4	T3-N2
△	0.60	2.4	T3-N3

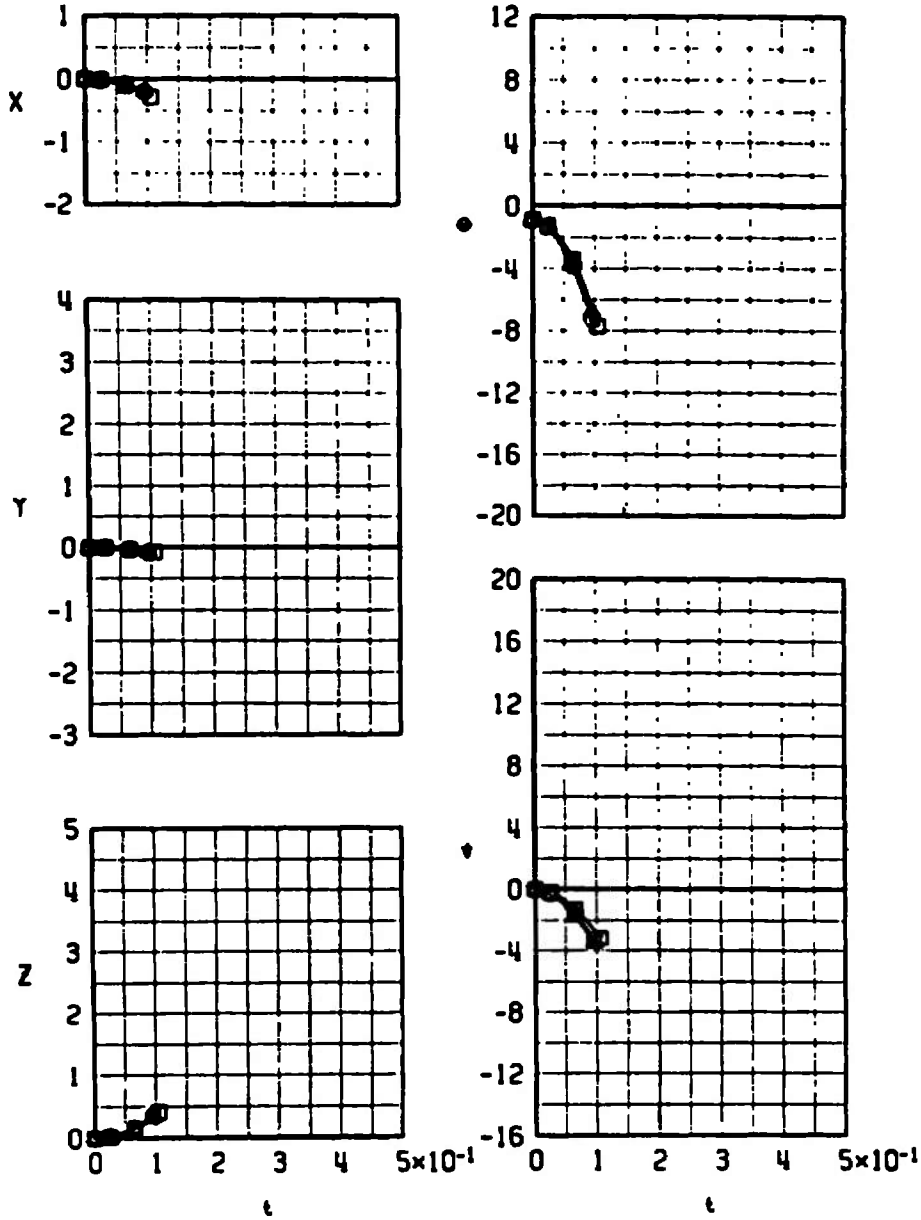


a.  $M_\infty = 0.60$

Fig. 14 Effect of Nose Geometry Variation on the Separation Trajectories of the Modular Weapon Store with Tail T3, Configuration 1R

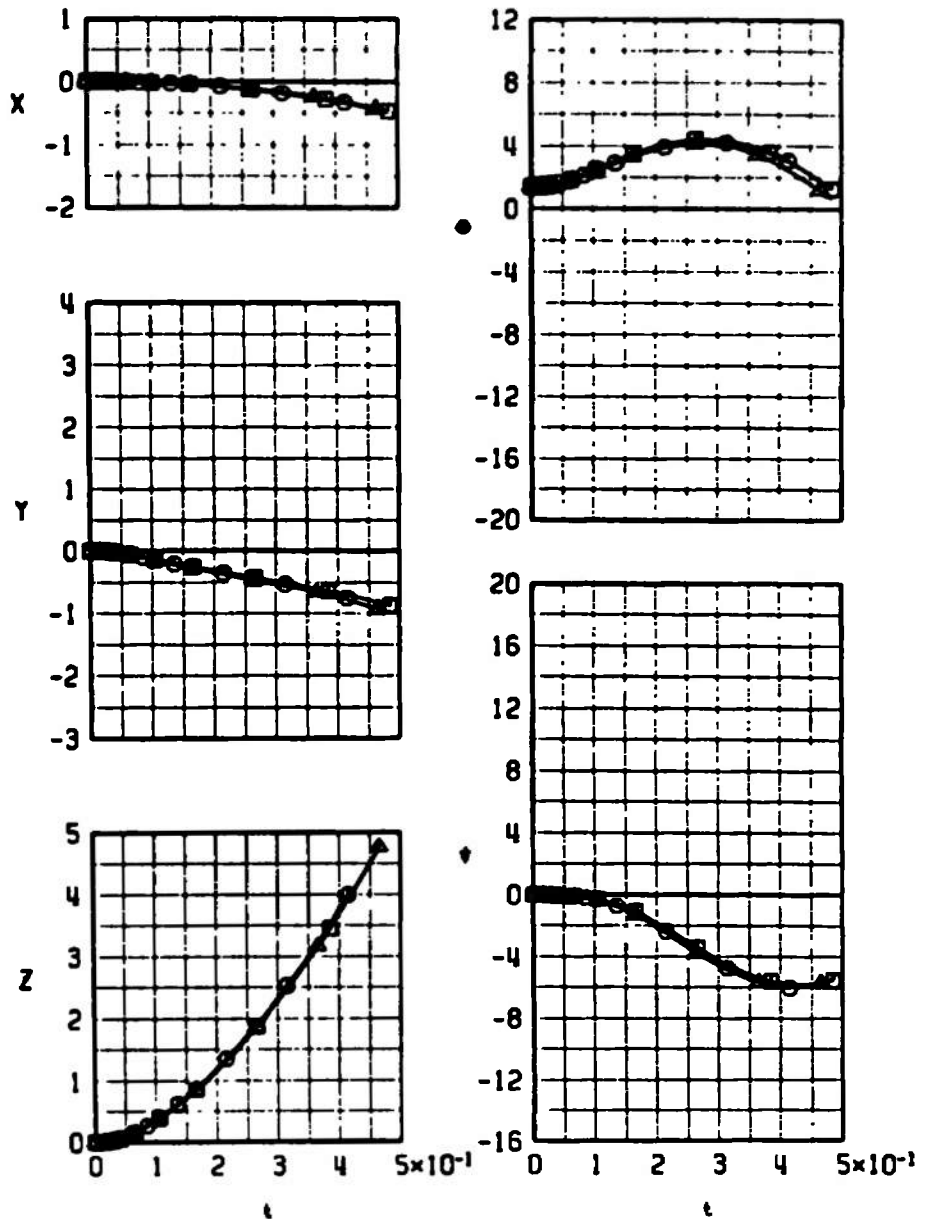
SYMBOL	$M_\infty$	$\alpha$	MODEL
□*	1.20	0.1	T3-N1
○*	1.20	0.1	T3-N2
△*	1.20	0.1	T3-N3

\*STORE-TO-PARENT CONTACT



b.  $M_\infty = 1.20$   
 Fig. 14 Concluded

SYMBOL	$M_\infty$	$\alpha$	MODEL
□	0.60	2.4	T4-N1
○	0.60	2.4	T4-N2
△	0.60	2.4	T4-N3

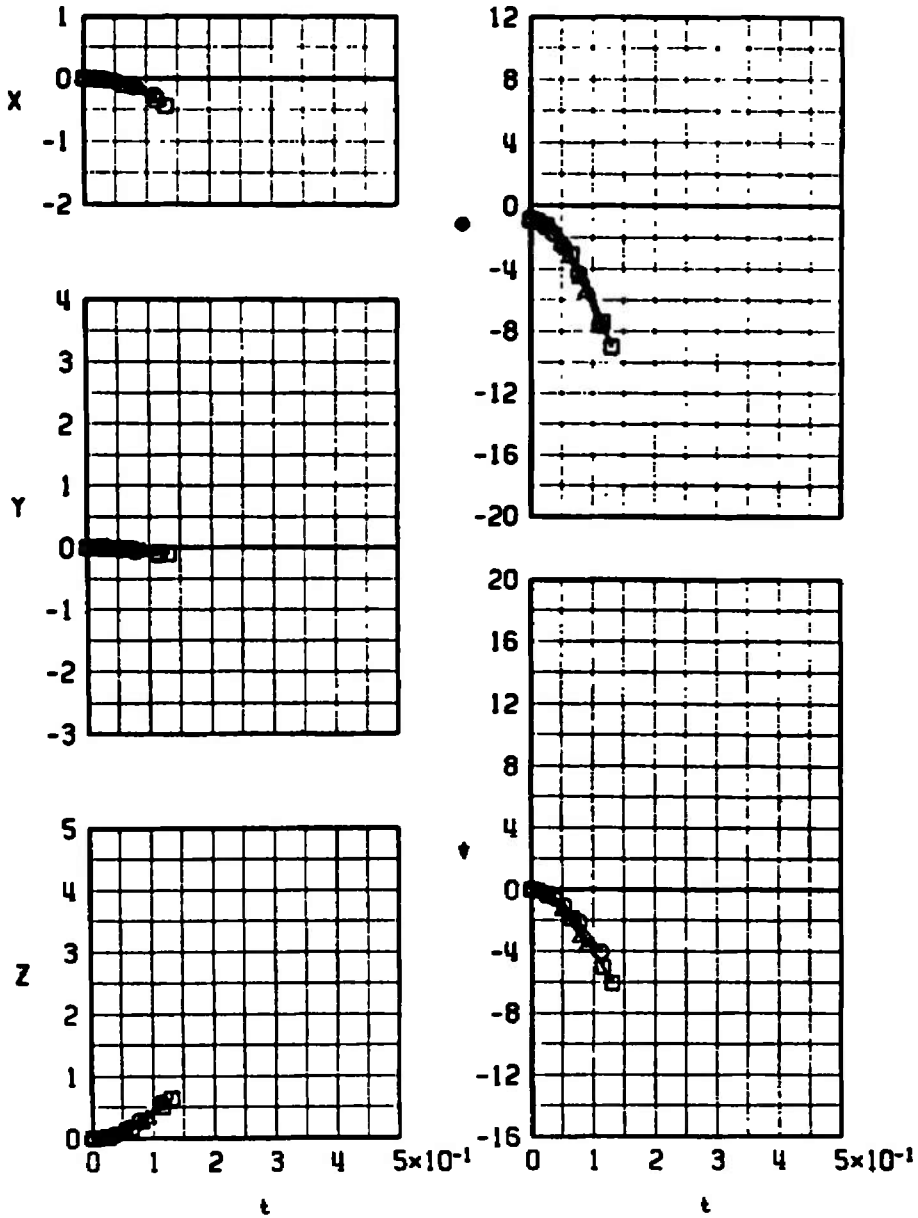


a.  $M_\infty = 0.60$

Fig. 15 Effect of Nose Geometry Variation on the Separation Trajectories of the Modular Store with Tail T4, Configuration 1R

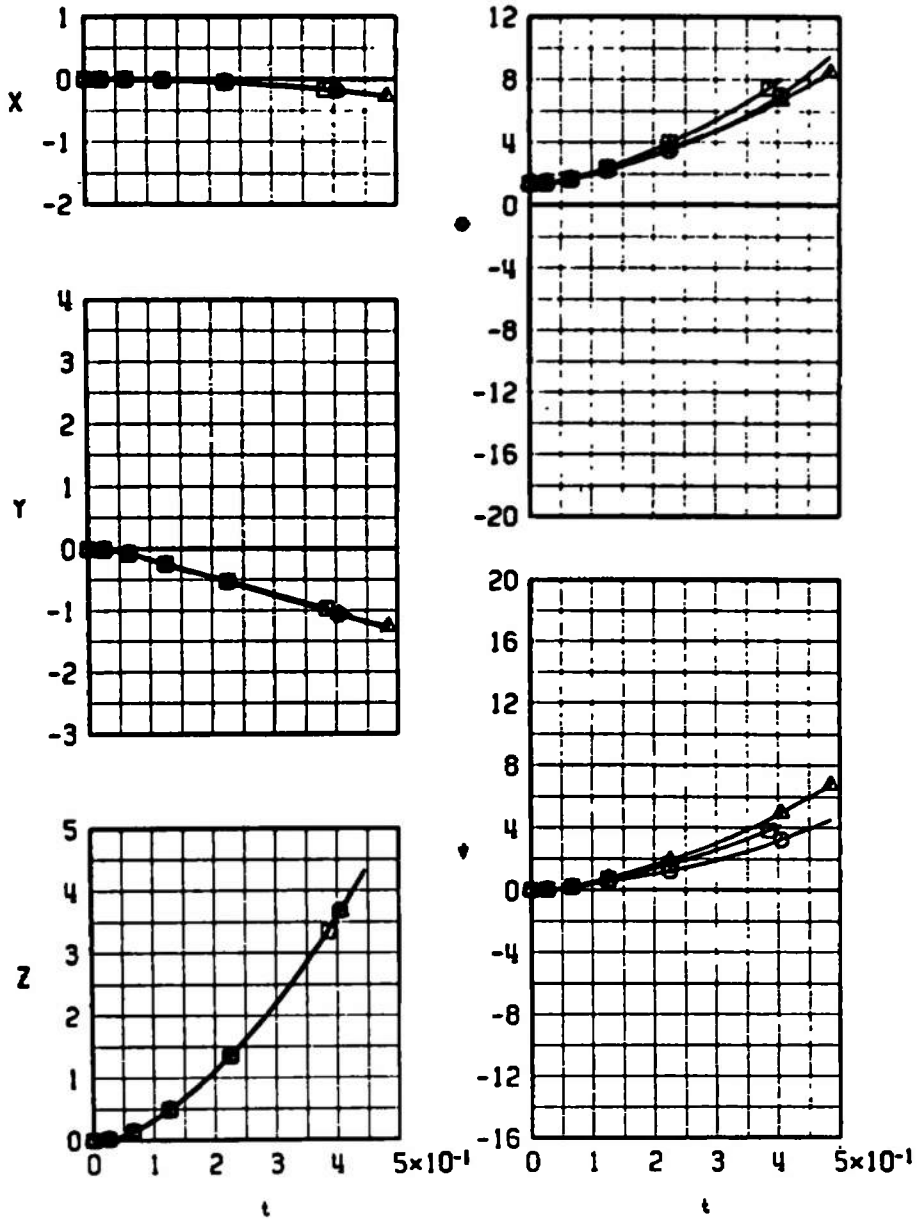
SYMBOL	$M_\infty$	$\alpha$	MODEL
□*	1.20	0.1	T4-N1
○*	1.20	0.1	T4-N2
△*	1.20	0.1	T4-N3

\*STORE-TO-PARENT CONTACT



b.  $M_\infty = 1.20$   
 Fig. 15 Concluded

SYMBOL	$M_\infty$	$\alpha$	MODEL
□	0.60	2.4	T1-N1
○	0.60	2.4	T1-N2
△	0.60	2.4	T1-N3

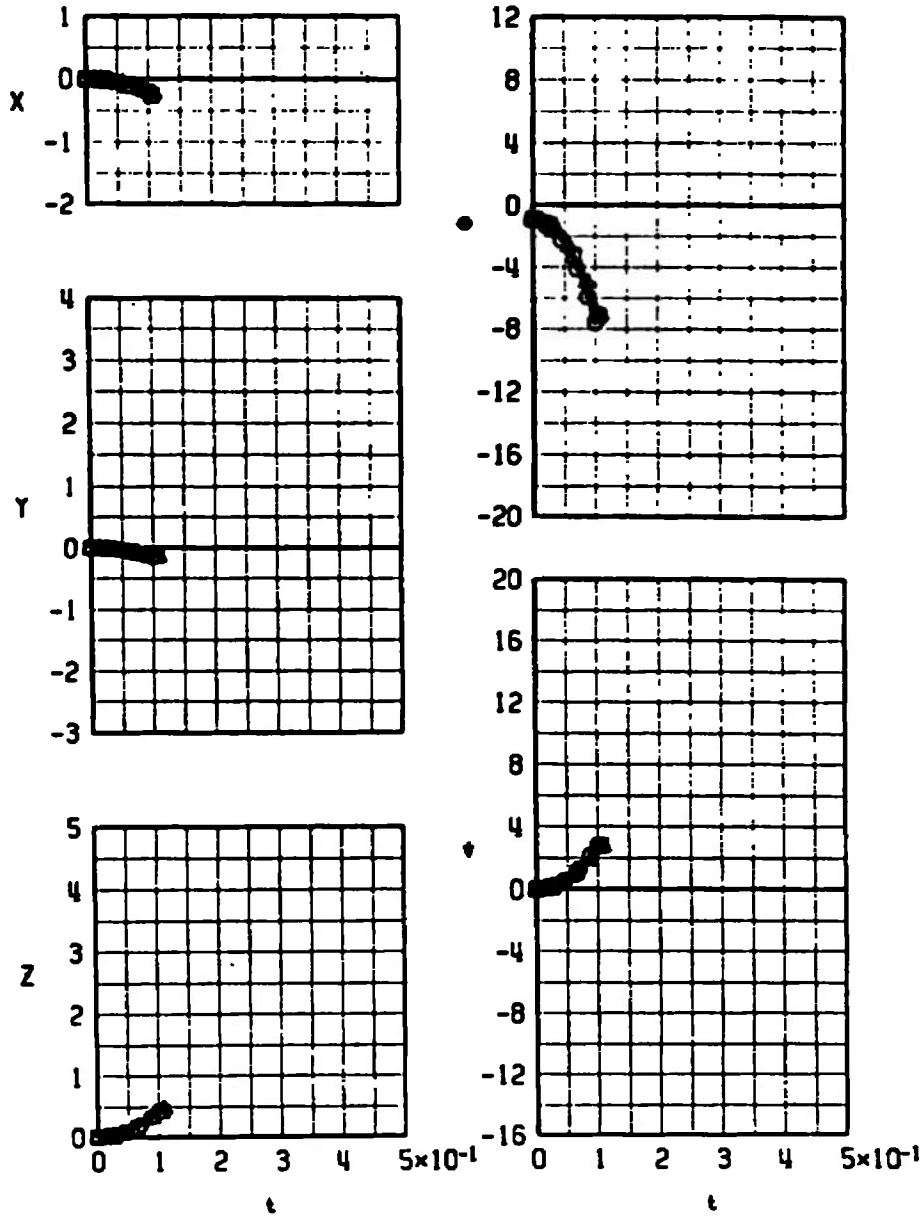


a.  $M_\infty = 0.60$

Fig. 16 Effect of Nose Geometry Variation on the Separation Trajectories of the Modular Weapon Stores with Tail T1, Configuration 1L

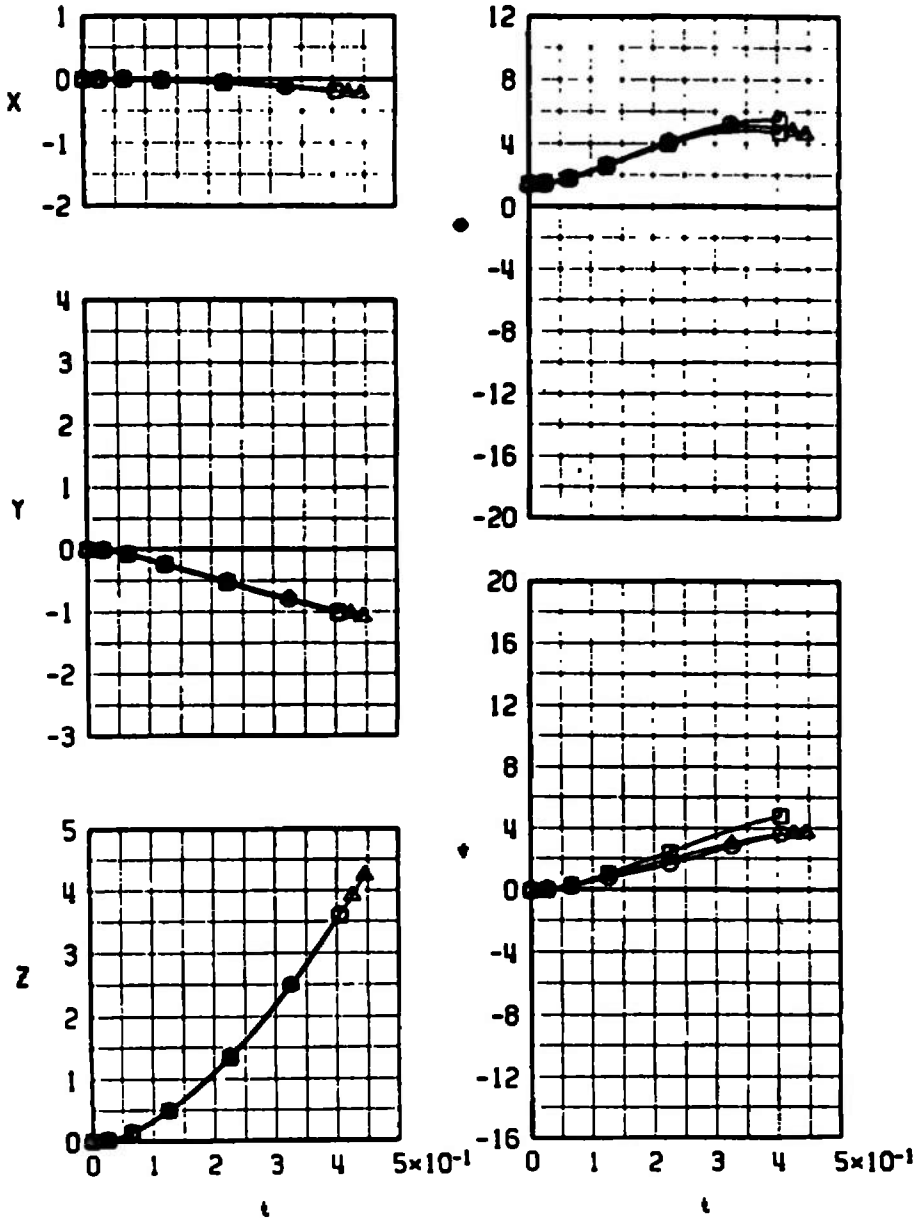
SYMBOL	$M_\infty$	$\alpha$	MODEL
□*	1.20	0.1	T1-N1
○*	1.20	0.1	T1-N2
△*	1.20	0.1	T1-N3

\*STORE-TO-PARENT CONTACT



b.  $M_\infty = 1.20$   
 Fig. 16 Concluded

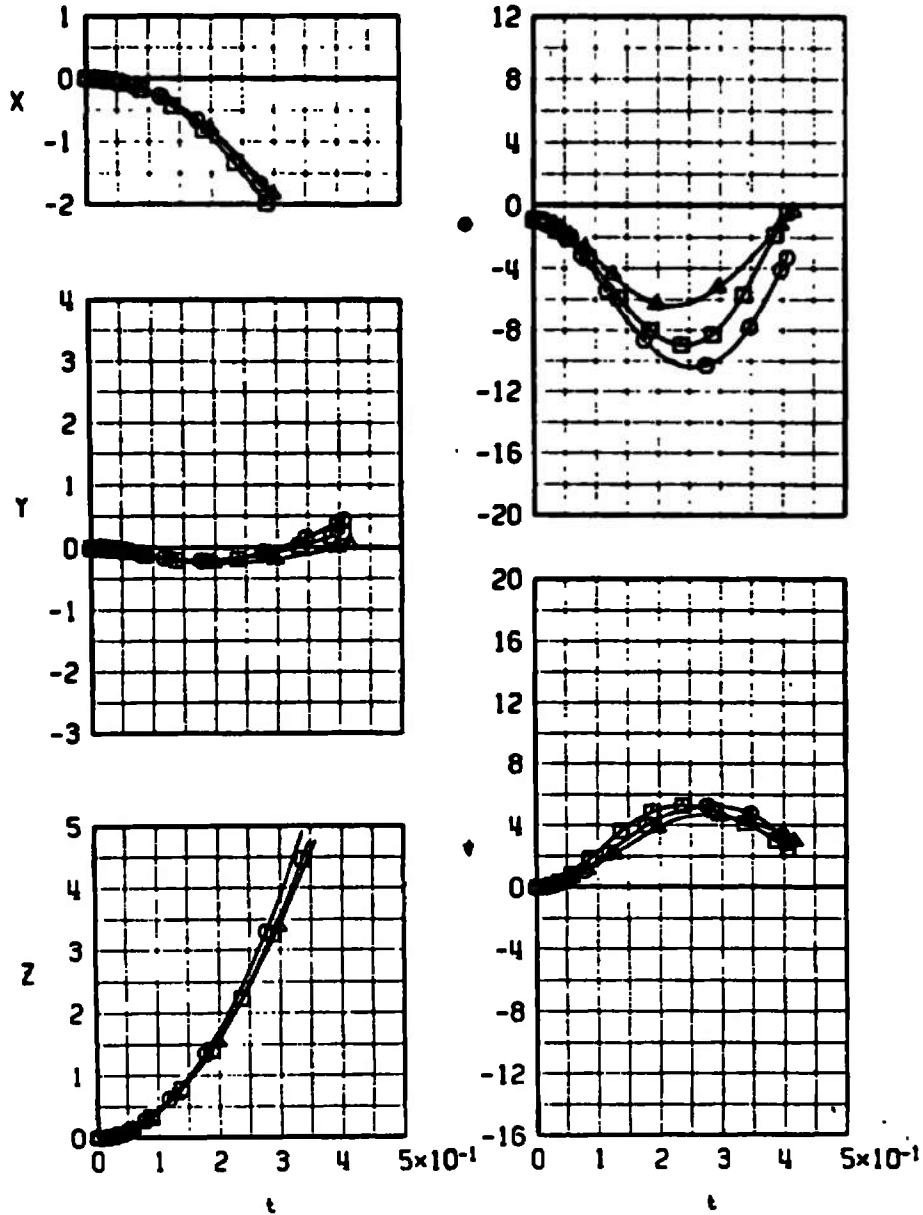
SYMBOL	$M_\infty$	$\alpha$	MODEL
□	0.60	2.4	T2-N1
○	0.60	2.4	T2-N2
△	0.60	2.4	T2-N3



a.  $M_\infty = 0.60$

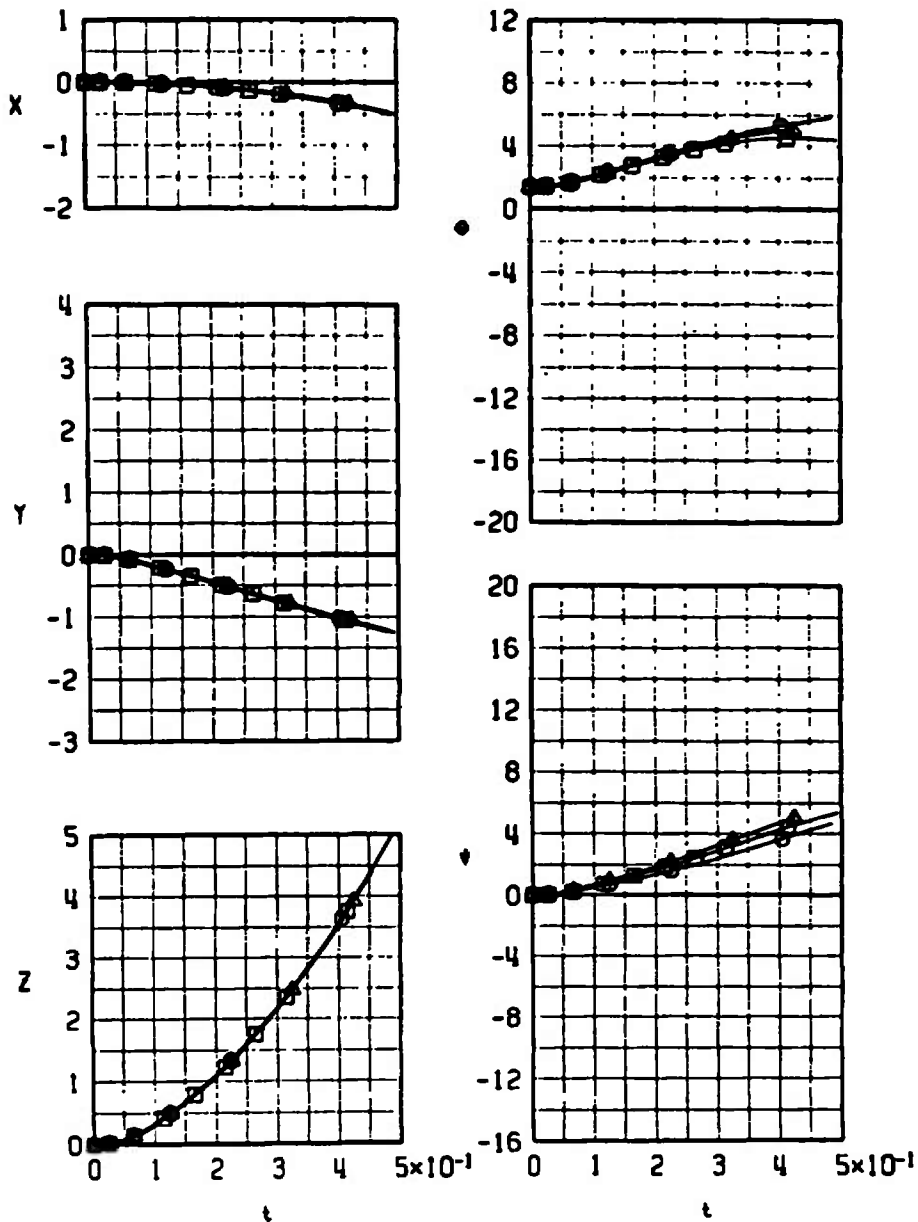
Fig. 17 Effect of Nose Geometry Variation on the Separation Trajectories of the Modular Weapon Stores with Tail T2, Configuration 1L

SYMBOL	$M_\infty$	$\alpha$	MODEL
□	1.20	0.1	T2-N1
○	1.20	0.1	T2-N2
△	1.20	0.1	T2-N3



b.  $M_\infty = 1.20$   
 Fig. 17 Concluded

SYMBOL	$M_\infty$	$\alpha$	MODEL
□	0.60	2.4	T3-N1
○	0.60	2.4	T3-N2
△	0.60	2.4	T3-N3

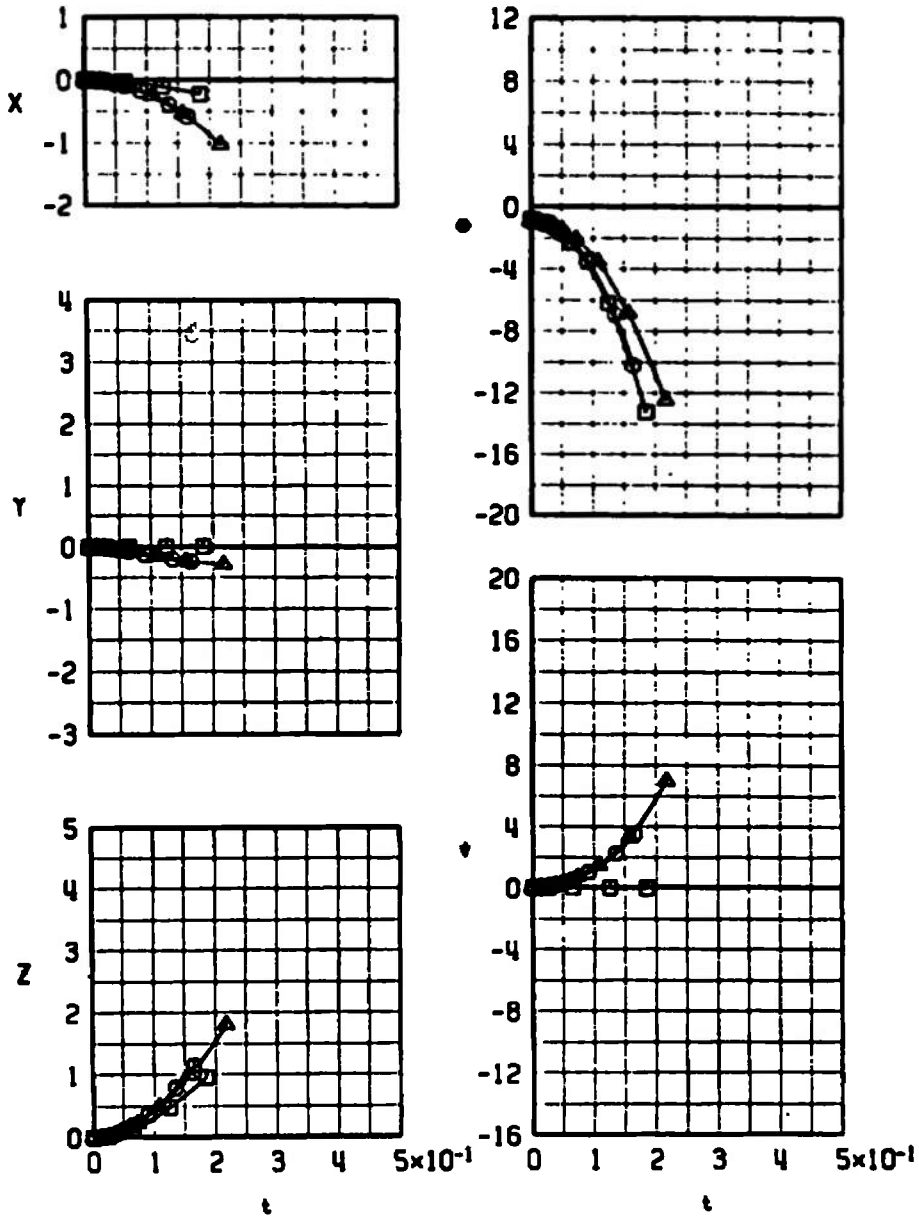


a.  $M_\infty = 0.60$

Fig. 18 Effect of Nose Geometry Variation on the Separation Trajectories of the Modular Weapon Stores with Tail T3, Configuration 1L

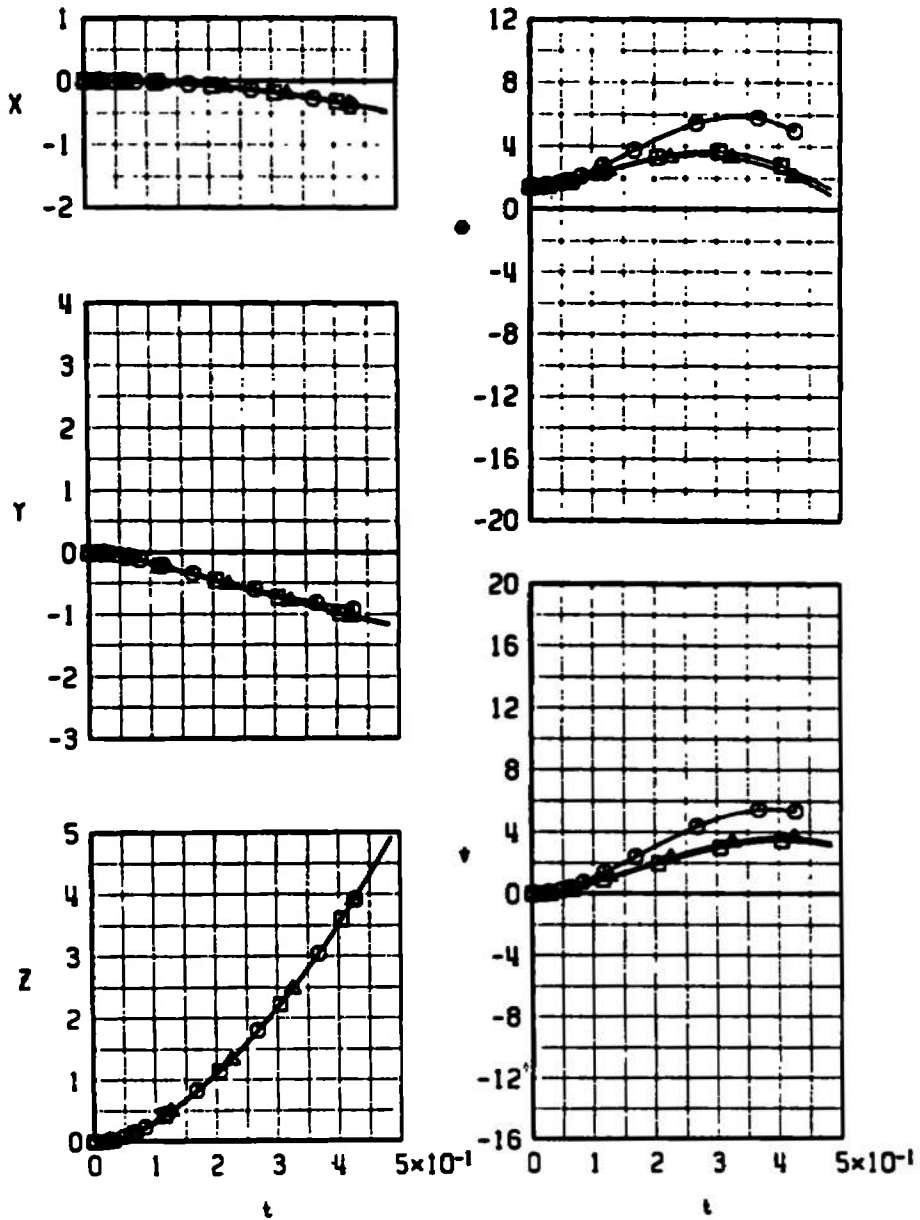
SYMBOL	$M_\infty$	$\alpha$	MODEL
□*	1.20	0.1	T3-N1
○*	1.20	0.1	T3-N2
△*	1.20	0.1	T3-N3

\*STORE-TO-PARENT CONTACT



b.  $M_\infty = 1.20$   
 Fig. 18 Concluded

SYMBOL	$M_0$	$\alpha$	MODEL
□	0.60	2.4	T4-N1
○	0.60	2.4	T4-N2
△	0.60	2.4	T4-N3

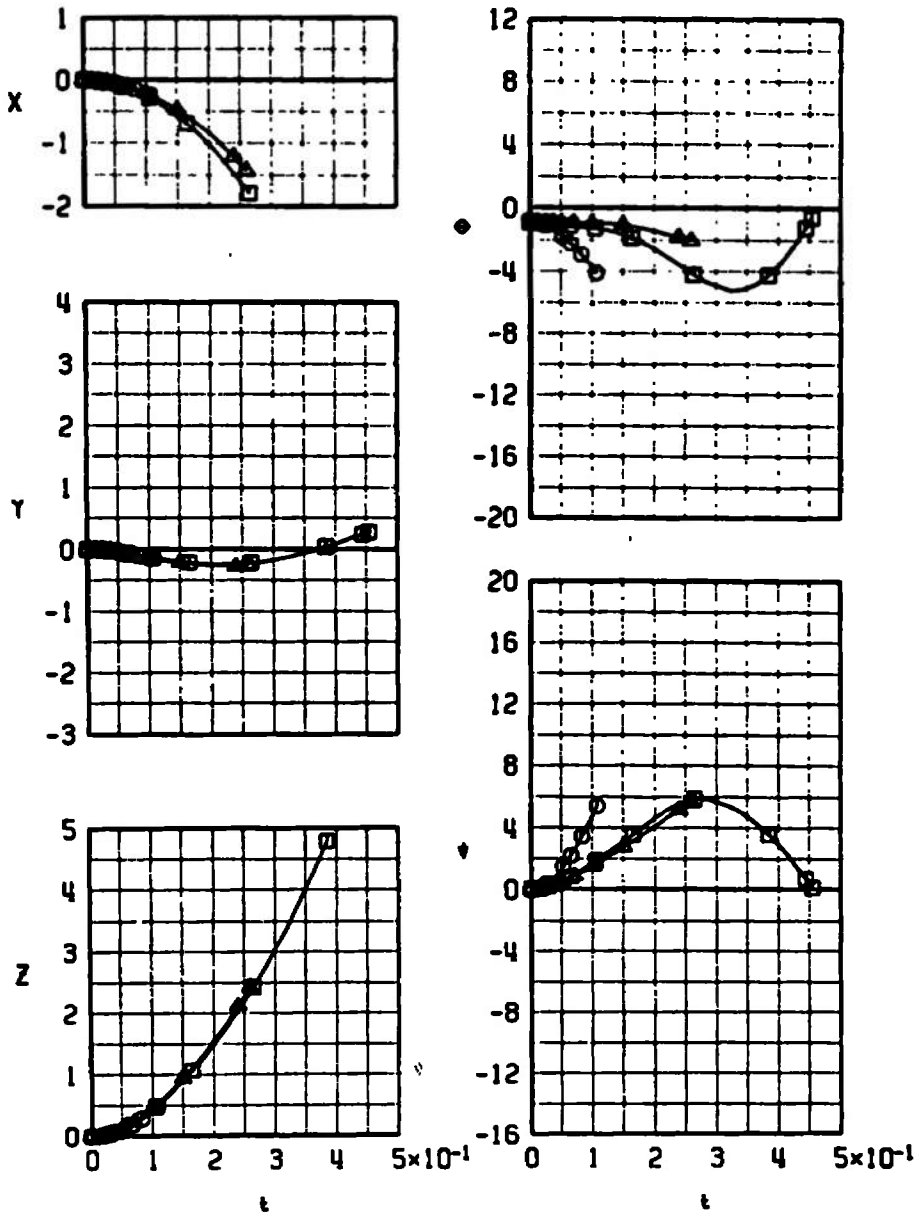


a.  $M_\infty = 0.60$

Fig. 19 Effect of Nose Geometry Variation on the Separation Trajectories of the Modular Weapon Stores with Tail T4, Configuration 1L

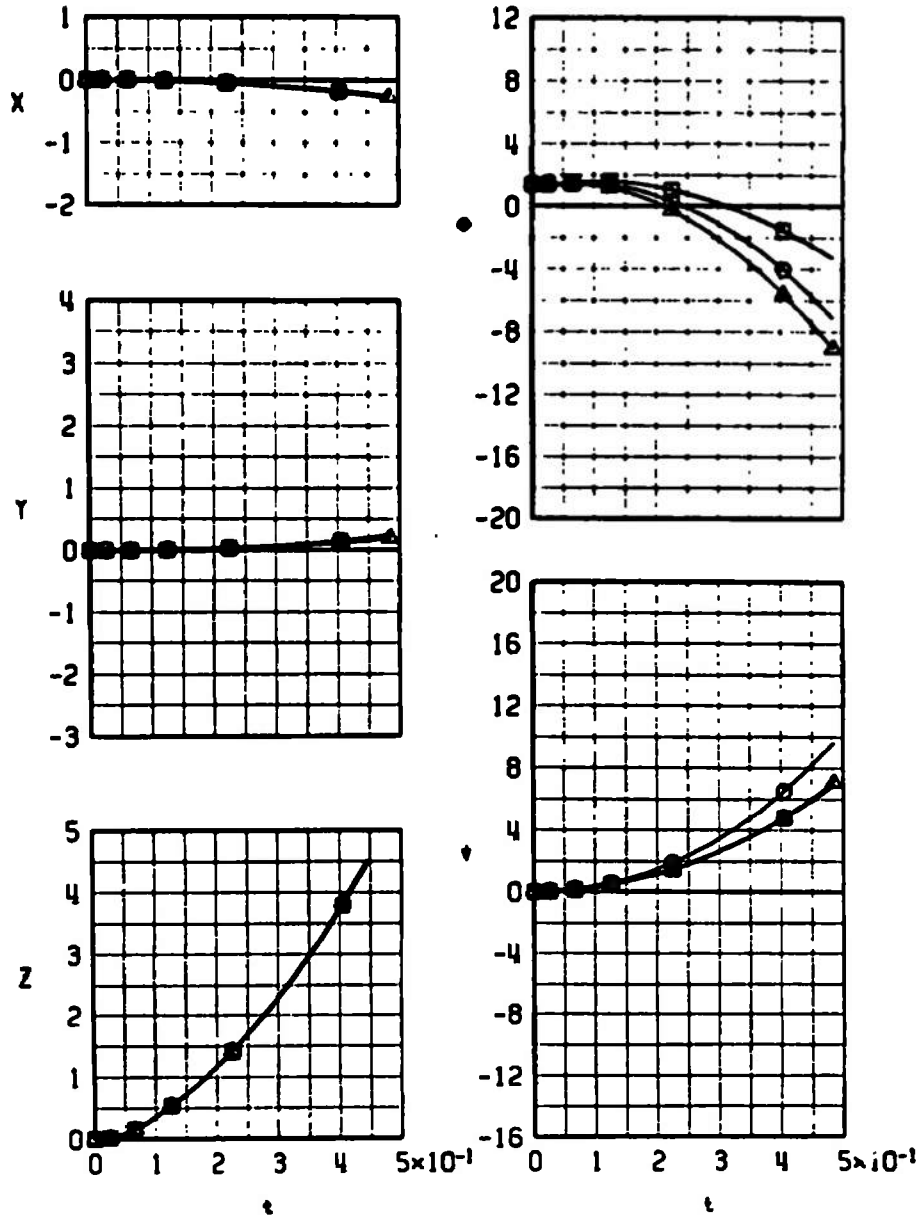
SYMBOL	$M_\infty$	$\alpha$	MODEL
□	1.20	0.1	T4-N1
○*	1.20	0.1	T4-N2
△	1.20	0.1	T4-N3

\*STORE-TO-PARENT CONTACT



b.  $M_\infty = 1.20$   
 Fig. 19 Concluded

SYMBOL	$M_\infty$	$\alpha$	MODEL
□	0.60	2.4	T1-N1
○	0.60	2.4	T1-N2
△	0.60	2.4	T1-N3

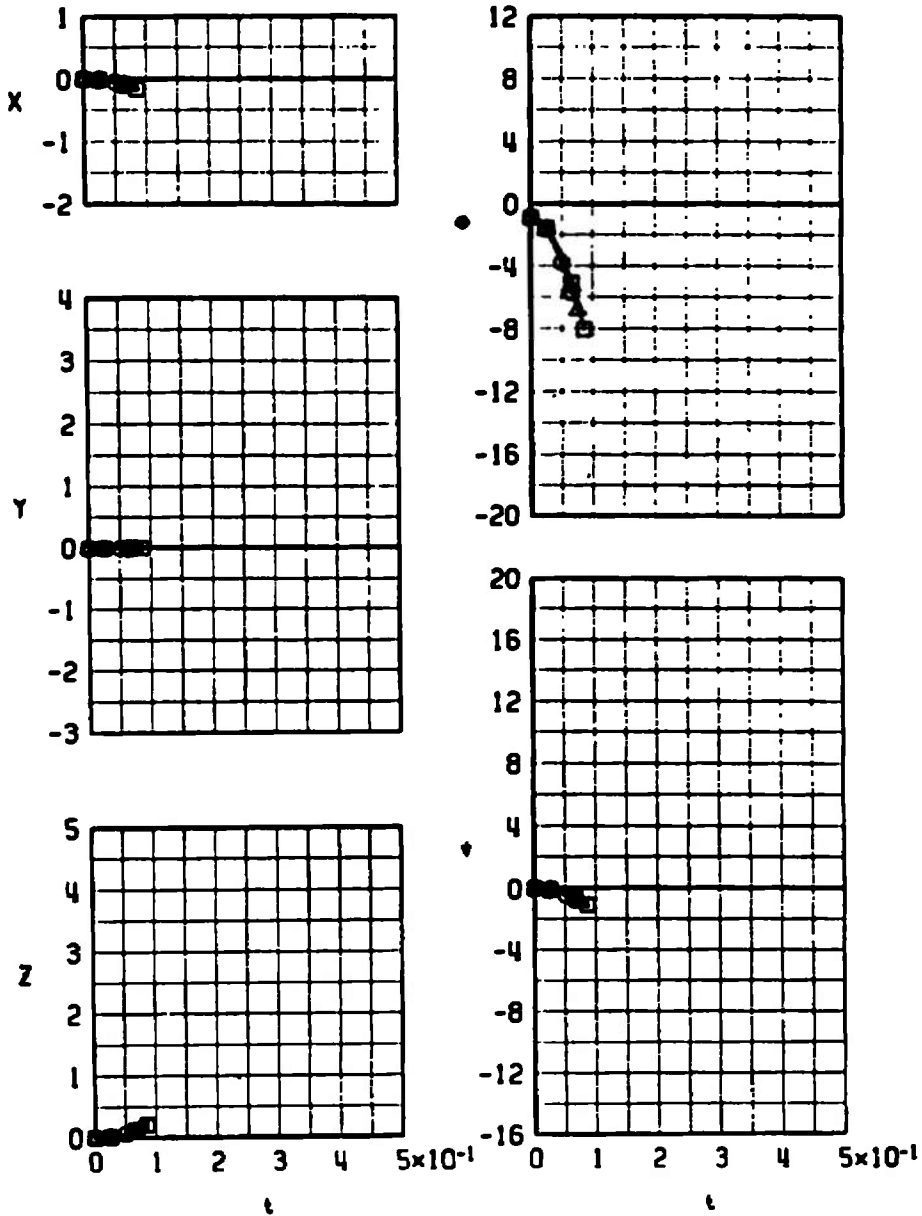


a.  $M_\infty = 0.60$

Fig. 20 Effect of Nose Geometry Variation on the Separation Trajectories of the Modular Weapon Stores with Tail T1, Configuration 2R

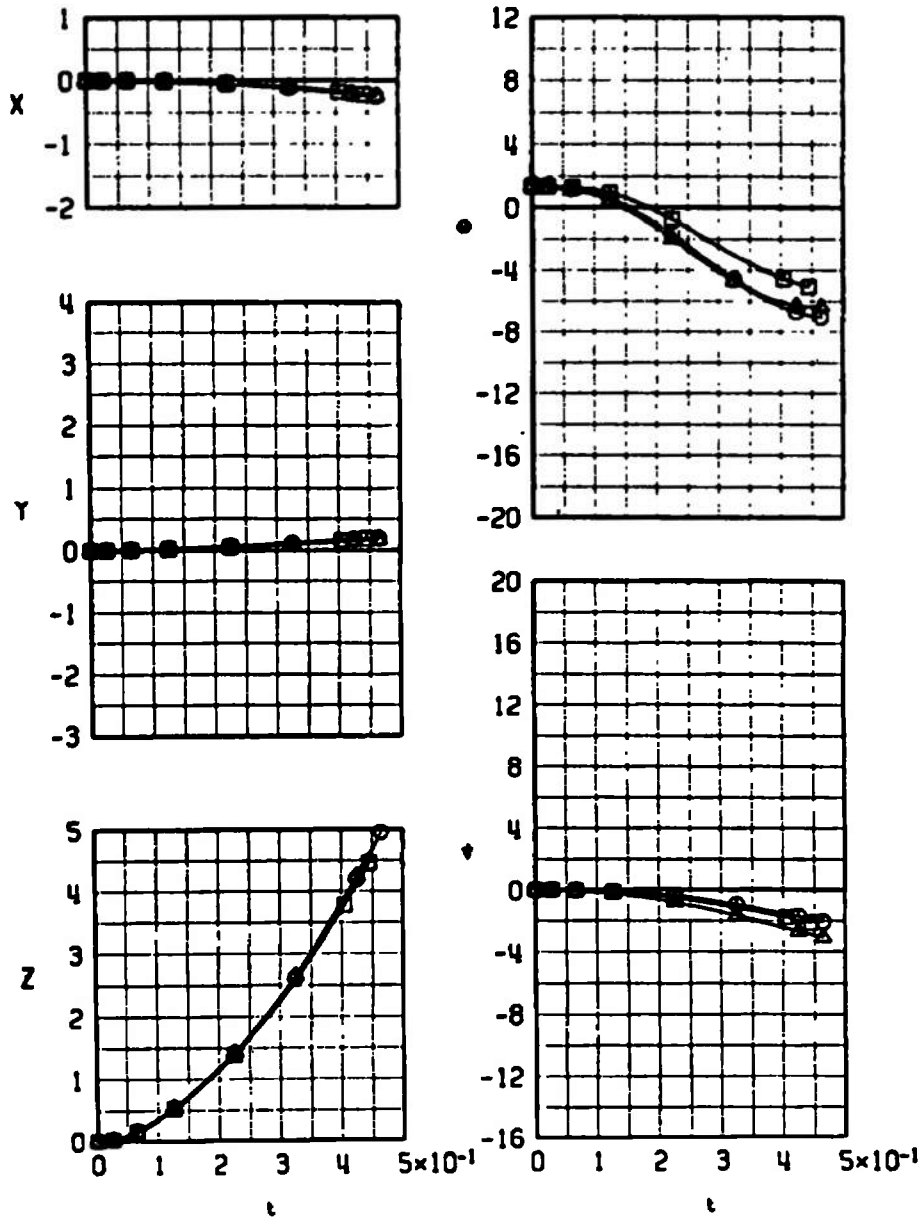
SYMBOL	$M_\infty$	$\alpha$	MODEL
□*	1.20	0.1	T1-N1
○*	1.20	0.1	T1-N2
△*	1.20	0.1	T1-N3

\*STORE-TO-PARENT CONTACT



b.  $M_\infty = 1.20$   
 Fig. 20 Concluded

SYMBOL	$M_\infty$	$\alpha$	MODEL
□	0.60	2.4	T2-N1
○	0.60	2.4	T2-N2
△	0.60	2.4	T2-N3

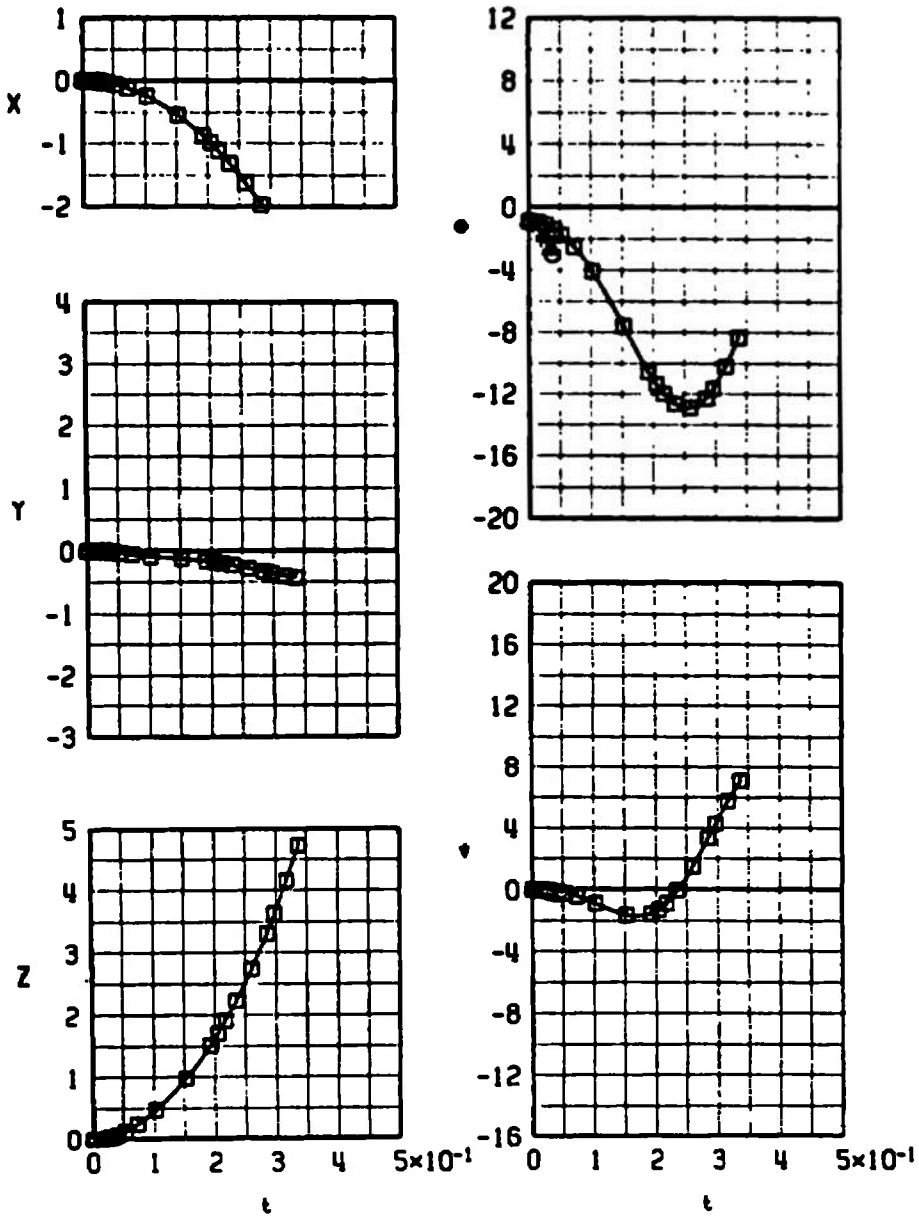


a.  $M_\infty = 0.60$

Fig. 21 Effect of Nose Geometry Variation on the Separation Trajectories of the Modular Weapon Stores with Tail T2, Configuration 2R

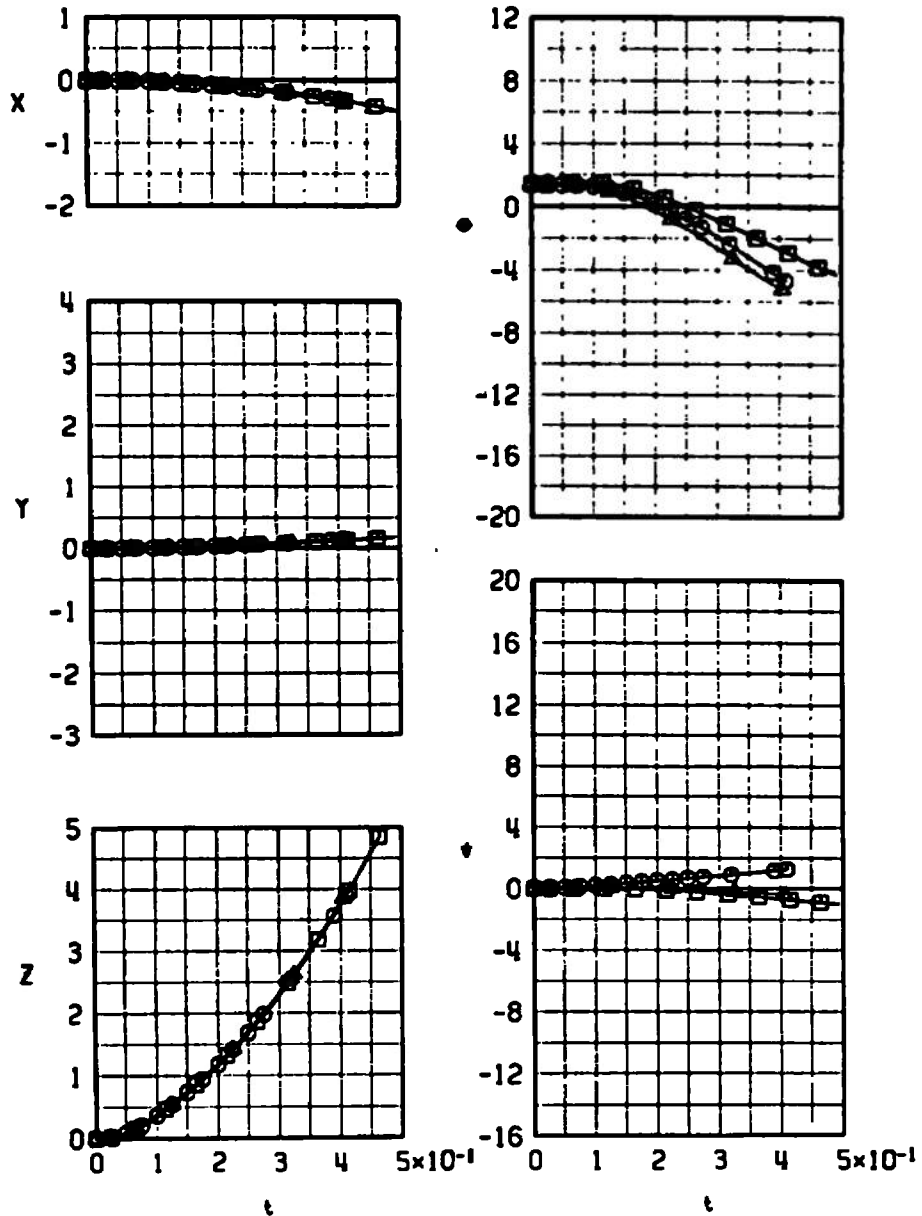
SYMBOL	$M_\infty$	$\alpha$	MODEL
□	1.20	0.1	T2-N1
○*	1.20	0.1	T2-N2
△*	1.20	0.1	T2-N3

\*STORE-TO-PARENT CONTACT



b.  $M_\infty = 1.20$   
 Fig. 21 Concluded

SYMBOL	$M_\infty$	$\alpha$	MODEL
□	0.60	2.4	T3-N1
○	0.60	2.4	T3-N2
△	0.60	2.4	T3-N3

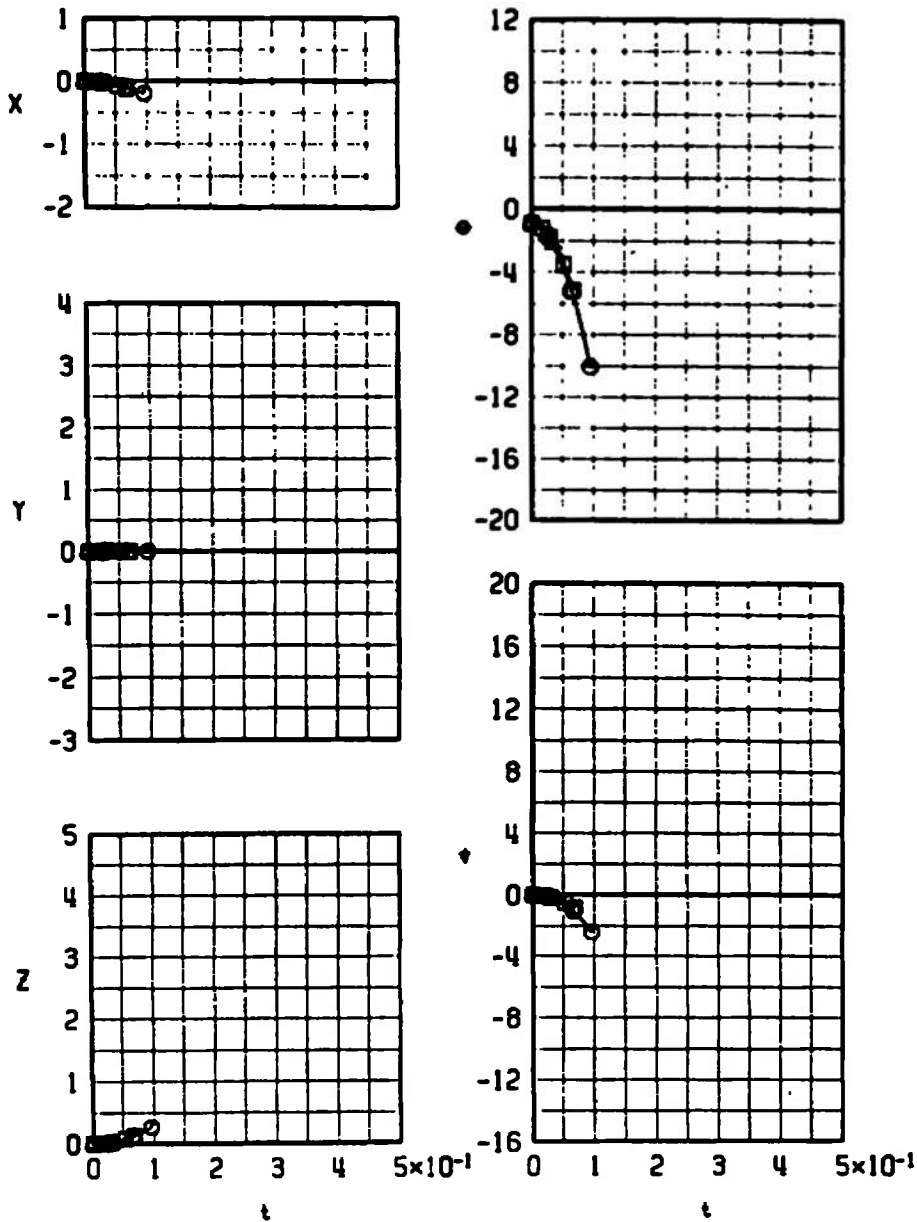


a.  $M_\infty = 0.60$

Fig. 22 Effect of Nose Geometry Variation on the Separation Trajectories of the Modular Weapon Stores with Tail T3, Configuration 2R

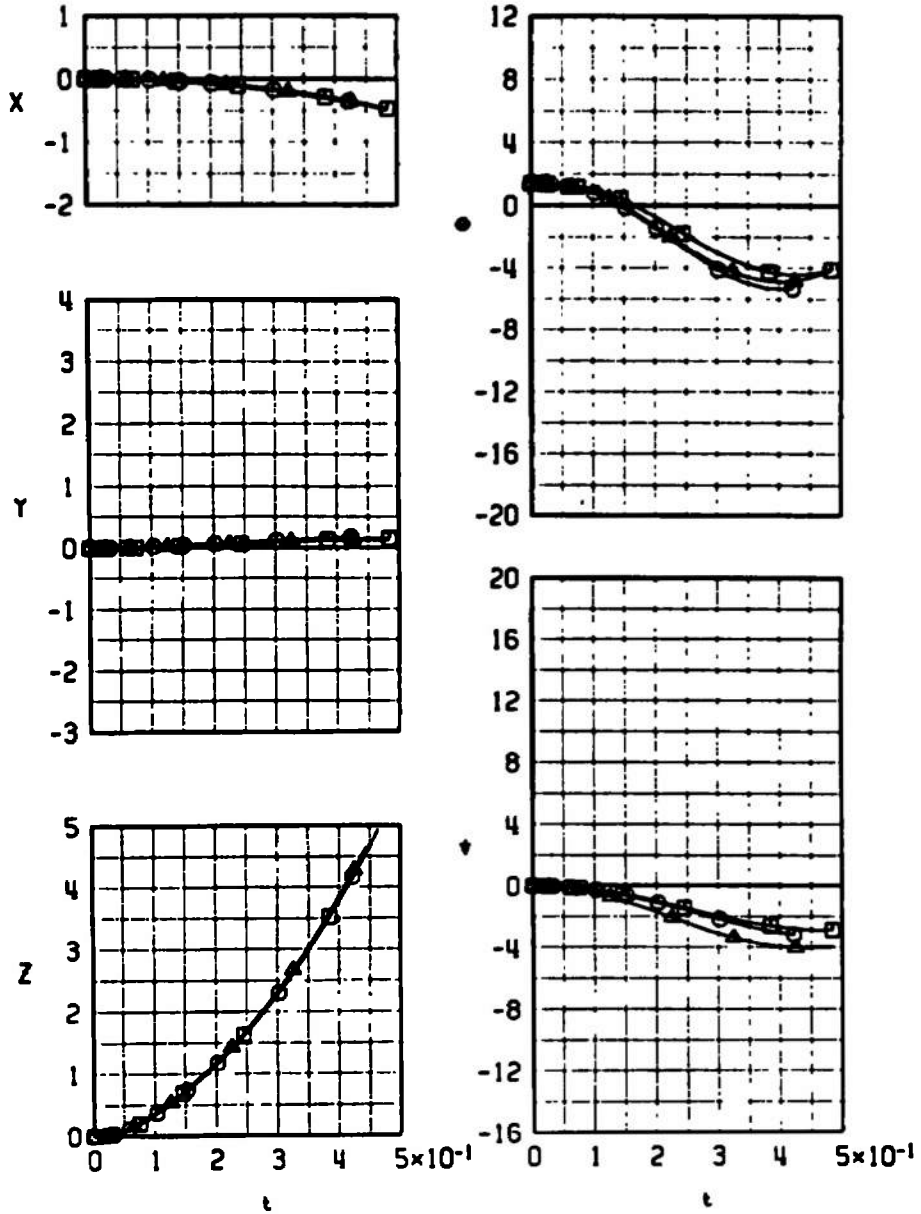
SYMBOL	$M_\infty$	$\alpha$	MODEL
□*	1.20	0.1	T3-N1
○*	1.20	0.1	T3-N2
△*	1.20	0.1	T3-N3

\*STORE-TO-PARENT CONTACT



b.  $M_\infty = 1.20$   
 Fig. 22 Concluded

SYMBOL	$M_\infty$	$\alpha$	MODEL
□	0.60	2.4	T4-N1
○	0.60	2.4	T4-N2
△	0.60	2.4	T4-N3

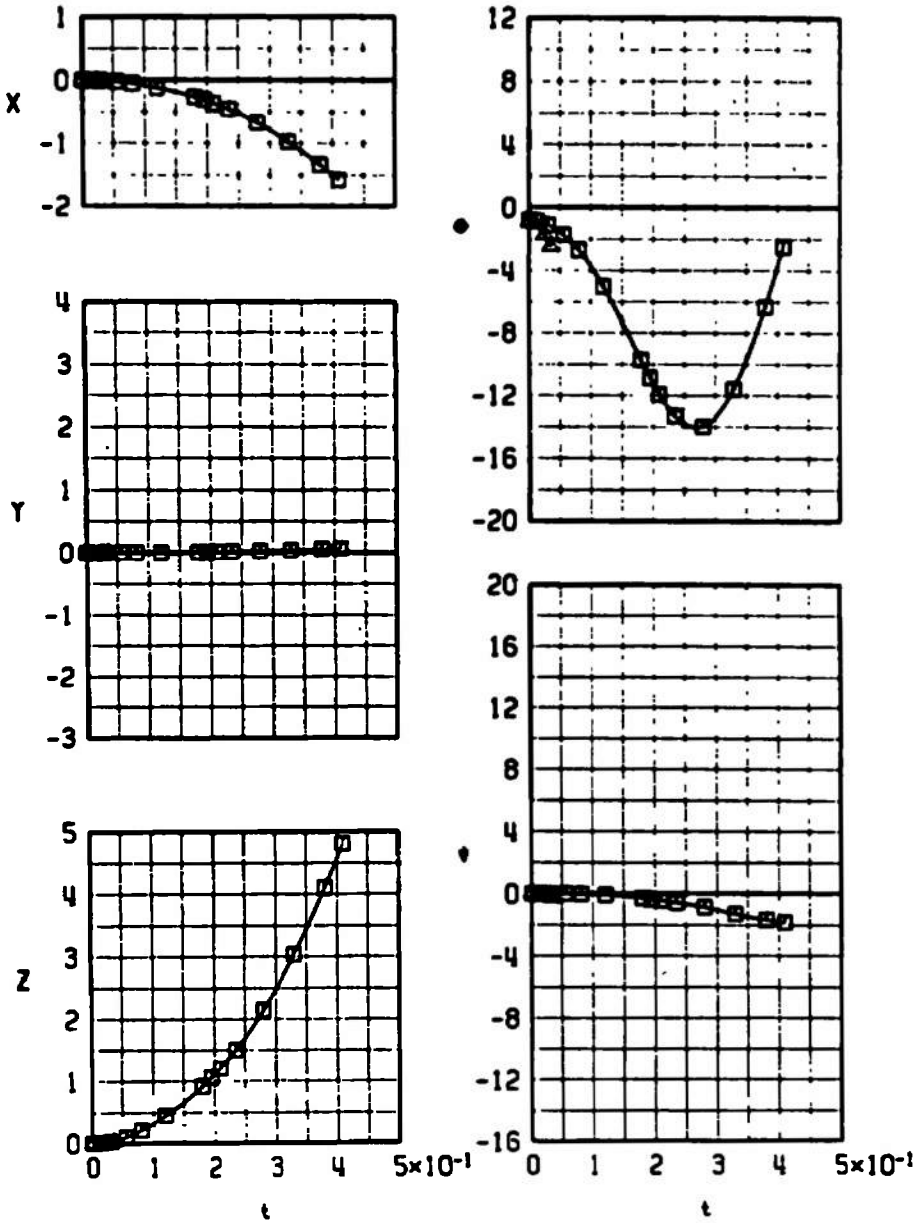


a.  $M_\infty = 0.60$

Fig. 23 Effect of Nose Geometry Variation on the Separation Trajectories of the Modular Weapon Stores with Tail T4, Configuration 2R

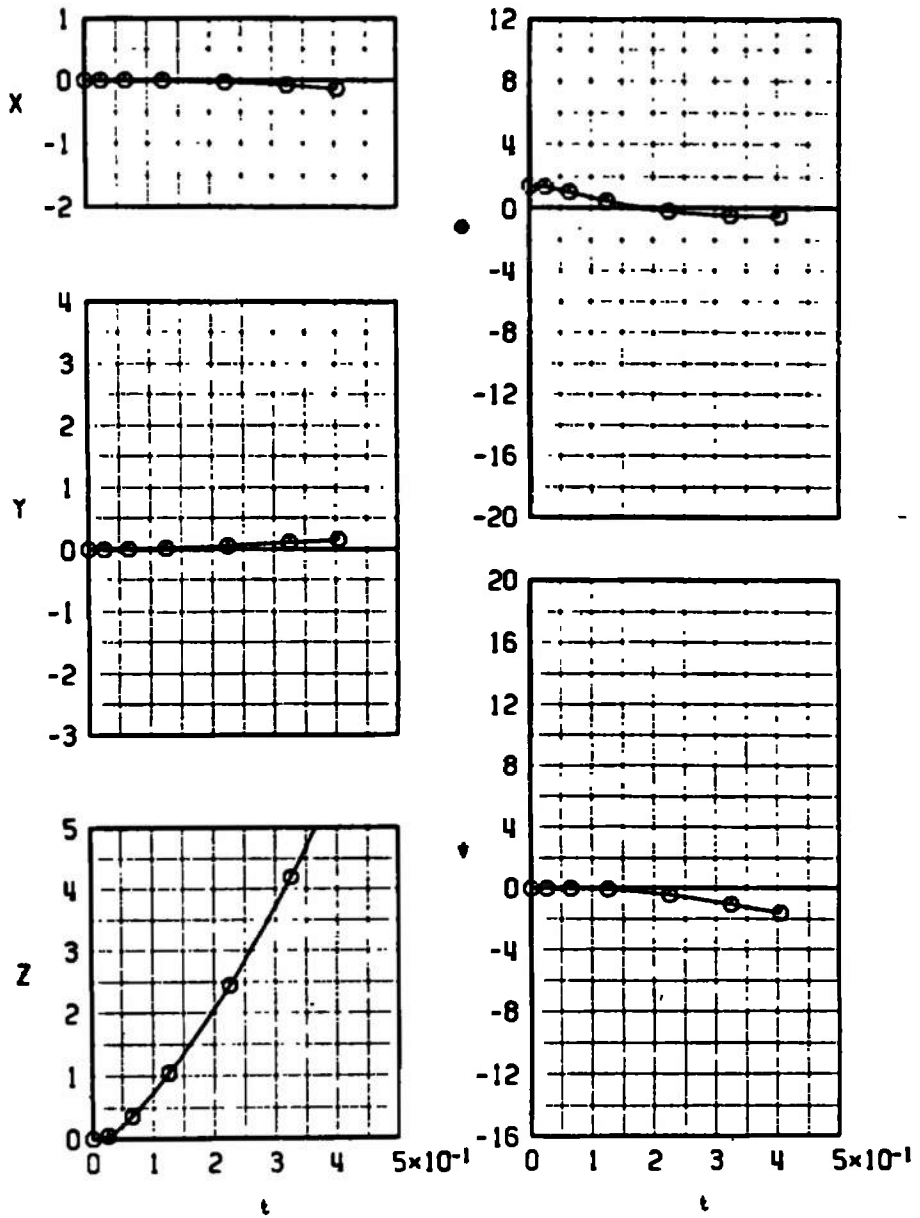
SYMBOL	$M_\infty$	$\alpha$	MODEL
□*	1.20	0.2	T4-N1
△*	1.20	0.2	T4-N3

\*STORE-TO-PARENT CONTACT



b.  $M_\infty = 1.20$   
 Fig. 23 Concluded

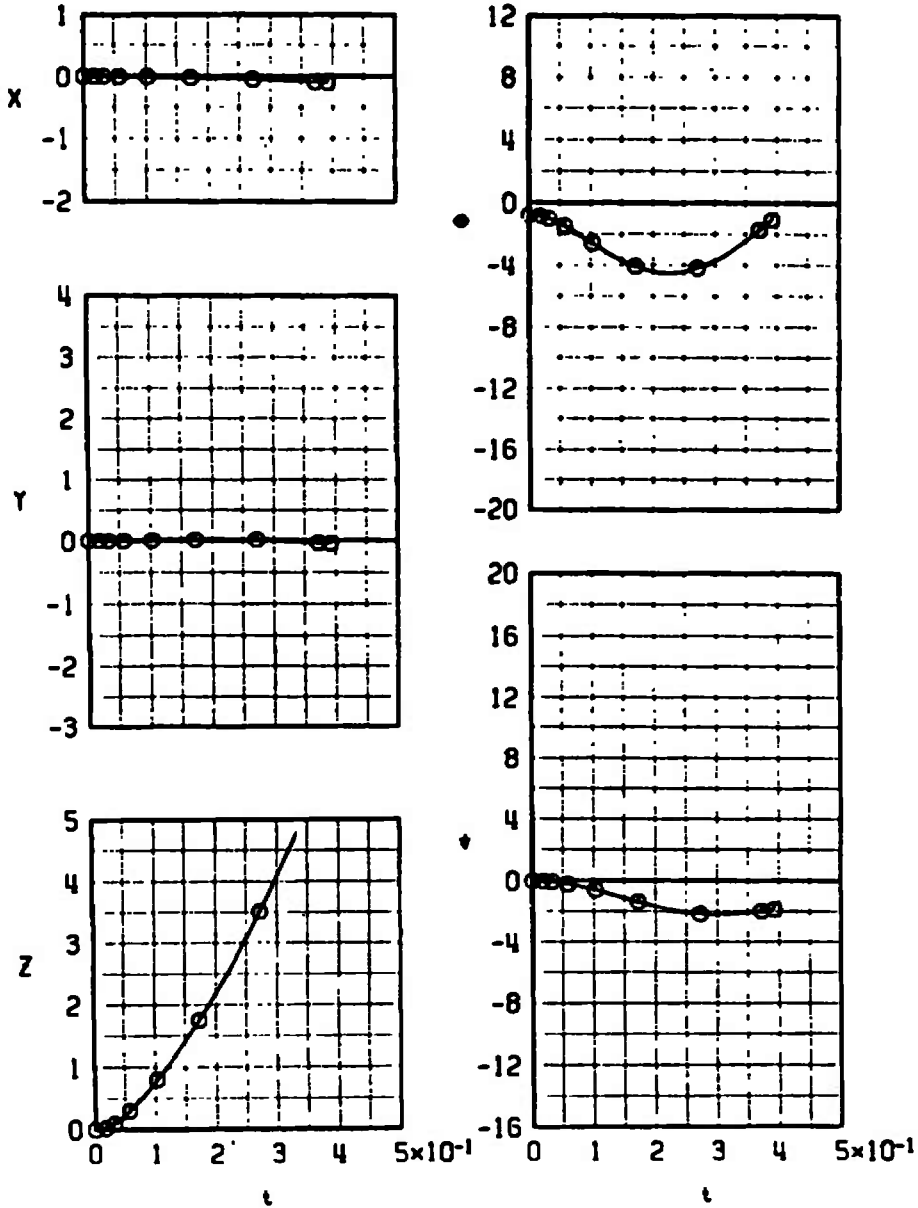
SYMBOL	$M_\infty$	$\alpha$	MODEL
O	0.60	2.4	T2-N1



a.  $M_\infty = 0.60$

Fig. 24 Separation Trajectories of the Modular Weapon Store with Nose N1 and Tail T2 from the Inboard Pylon, Configuration 3R

SYMBOL	$M_\infty$	$\alpha$	MODEL
O	0.90	0.2	T2-N1



b.  $M_\infty = 0.90$   
 Fig. 24 Concluded

**TABLE I**  
**FULL-SCALE STORE PARAMETERS**  
**USED IN TRAJECTORY CALCULATIONS**

Parameter	All Store Combinations
$\bar{m}$	25.0500
$X_{cg}$	2.5167
$I_{xx}$	4.000
$I_{yy}$	65.200
$I_{zz}$	65.20
b	1.0000
S	0.78540
Ejector Piston Distance Forward of Store cg <hr style="width: 20%; margin: 0 auto;"/>	
1. $X_L$ , TER	-0.1719
2. $X_{L1}$ , MAV 12	0.8333
3. $X_{L2}$ , MAV 12	-0.8333

**TABLE II  
DAMPING COEFFICIENTS USED IN TRAJECTORY CALCULATIONS**

Tail		T1	T2	T3	T4
Nose	N1	-15.0	-23.0	-21.0	-34.0
	N2	-15.0	-26.0	-24.0	-37.0
	N3	-18.0	-26.0	-24.0	-37.0
$C_{lp}$					
---		-1.0	-2.0	-1.0	-3.0

**TABLE III  
AXIAL-FORCE COEFFICIENTS,  $C_A$ , USED IN FULL-SCALE  
TRAJECTORY CALCULATIONS**

Nose and Tail Combinations				
$M_\infty$	N1, T1, T2	N2, N3 T1, T2	N1, T3, T4	N2, N3 T3, T4
0.60	0.18	0.18	0.30	0.30
0.90	0.40	0.40	0.50	0.50
1.20	0.80	0.70	0.90	0.74

TABLE IV  
F-4C LOAD CONFIGURATIONS

CONFIG. NO.	OUTB'D	INB'D	CONFIG. NO.	INB'D	OUTB'D
1L	○ 370-GAL FUEL TANK	●▽	1R	●▽○	○ 370-GAL FUEL TANK
2L	○ 370-GAL FUEL TANK	▽	2R	○▽○ ●	○ 370-GAL FUEL TANK
3L	○ 370-GAL FUEL TANK	▽	3R	●	○ 370-GAL FUEL TANK

○ DENOTES DUMMY STORE

▽ DENOTES TER

● DENOTES STING MOUNTED STORE

UNCLASSIFIED

Security Classification

DOCUMENT CONTROL DATA - R & D

(Security classification of title, body of abstract and indexing annotation must be entered when the overall report is classified)

1 ORIGINATING ACTIVITY (Corporate author) Arnold Engineering Development Center Arnold Air Force Station, Tennessee 37389	2a. REPORT SECURITY CLASSIFICATION <b>UNCLASSIFIED</b>
	2b. GROUP N/A

3 REPORT TITLE  
**SEPARATION TRAJECTORIES OF MODULAR WEAPON STORES WITH VARIOUS NOSE AND TAIL GEOMETRIES FROM THE F-4C AIRCRAFT**

4 DESCRIPTIVE NOTES (Type of report and inclusive dates)  
**Final Report - July 19 to August 2, 1972**

5 AUTHOR(S) (First name, middle initial, last name)  
**David W. Hill, Jr., ARO, Inc.**

6 REPORT DATE <b>December 1972</b>	7a. TOTAL NO OF PAGES <b>57</b>	7b. NO OF REFS <b>0</b>
---------------------------------------	------------------------------------	----------------------------

8a CONTRACT OR GRANT NO  b PROJECT NO  c Program Element 63601F  d System 670D	9a. ORIGINATOR'S REPORT NUMBER(S) <b>AEDC-TR-72-182 AFATL-TR-72-220</b>
	9b. OTHER REPORT NO(S) (Any other numbers that may be assigned this report) <b>ARO-PWT-TR-72-163</b>

10 DISTRIBUTION STATEMENT **Distribution limited to U.S. Government agencies only; this report contains information on test and evaluation of military hardware; December 1972; other requests for this document must be referred to Air Force Armament Laboratory (DLJM), Eglin AFB, FL 32542.**

11 SUPPLEMENTARY NOTES <b>Available in DDC</b>	12. SPONSORING MILITARY ACTIVITY <b>Air Force Armament Laboratory (DLJM) Eglin AFB, Florida 32542</b>
---	--

13 ABSTRACT

Tests were conducted in the Aerodynamic Wind Tunnel (4T) using 0.05-scale models to investigate the separation characteristics of modular weapon configurations with different nose and tail geometries when released from various positions on the triple ejection rack at the wing inboard pylon location on the F-4C aircraft. Captive trajectory data were obtained for level flight at Mach numbers 0.6, 0.9, and 1.2 at a simulated altitude of 5000 ft. The parent aircraft angle of attack was varied from 0.1 to 2.4 deg, depending on Mach number. In general, for any nose and tail combination, the effect of increasing Mach number was to produce a more negative (nose down) initial pitch rate. For the configurations tested, and over the Mach number and trajectory intervals of this test, the modular weapon with a hemispherical nose and conical boattail appeared to be the most suitable store for separation without store-to-parent contact.

Distribution limited to U.S. Government agencies only; this report contains information on test and evaluation of military hardware; December 1972; other requests for this document must be referred to Air Force Armament Laboratory (DLJM), Eglin AFB, FL 32542.

14. KEY WORDS	LINK A		LINK B		LINK C	
	ROLE	WT	ROLE	WT	ROLE	WT
bombs (ordnance) F-4C aircraft trajectories separation characteristics transonic flow wind tunnel tests						

AFSC  
Area of AFB Term